HEADQUARTERS
QUARTERMASTER RESEARCH & ENGINEERING COMMANDING COMMAND
U S ARMY

TECHNICAL REPORT
PP-3

TENSILE IMPACT ON RUBBER AND NYLON) NYLON

QUARTERMASTER RESEARCH & ENGINEERING CENTER RING CENTER
PIONEERING RESEARCH DIVISION ION

MAY 1962

NATICK, MASSACHUSETTS MASSACHUSETTS

AD- Div. 25, 14, 24 Accession No.

Quartermaster Research & Engineering Center, Natick, Mass.
TENSILE IMPACT ON RUBBER AND NYLON by Malcolm N. Pilsworth, Jr., 70 pp. illus. (Technical Report PR-3) May 1962

A method has been sought of describing the response of visco-elastic materials to loading when the velocity of strain propagation in the material is the controlling factor. A machine is described that delivers a longitudinal impact at about 150 ft/sec to a yarn or strip. The impact is photographed using a high-speed stroboscope and a moving mirror. Strain-time-position data are obtained from the picture. Results are given for the impact of a rubber strip. In another experimental technique the force at the fixed end of a nylon yarn during impact is measured. Tentative high-speed stress-strain curves were deduced, for the rubber from the photograph and for the nylon from another series of tests in which the acceleration of a tail mass was measured. Assuming that these curves hold during the impact with no time dependency, the strain patterns were computed by a method of characteristics given by von Karman, and compared with the experimental results. The timing and strain levels of the measured pulses are well duplicated by the calculation. However, the calculated pulses have much steeper fronts than are observed. For both rubber and nylon, in order to describe the impact response it is necessary to include a creep function as well as a dynamic stress-strain curve. So far it has not been possible to analyze a photograph of an impact on nylon yarn; this is because of large variations of strain with position.

UNCLASSIFIED

1. Stresses
2. Nylon
3. Rubber
4. Creep
5. Dynamics
6. Elasticity
7. Photographic analysis
8. Plasticity
9. Polymers
10. Stroboscopes
I. Title
II. Series
III. Pilsworth, Malcolm N., Jr.

AD- Div. 25, 14, 24 Accession No.

Quartermaster Research & Engineering Center, Natick, Mass.
TENSILE IMPACT ON RUBBER AND NYLON by Malcolm N. Pilsworth, Jr., 70 pp. illus. (Technical Report PR-3) May 1962

A method has been sought of describing the response of visco-elastic materials to loading when the velocity of strain propagation in the material is the controlling factor. A machine is described that delivers a longitudinal impact at about 150 ft/sec to a yarn or strip. The impact is photographed using a high-speed stroboscope and a moving mirror. Strain-time-position data are obtained from the picture. Results are given for the impact of a rubber strip. In another experimental technique the force at the fixed end of a nylon yarn during impact is measured. Tentative high-speed stress-strain curves were deduced, for the rubber from the photograph and for the nylon from another series of tests in which the acceleration of a tail mass was measured. Assuming that these curves hold during the impact with no time dependency, the strain patterns were computed by a method of characteristics given by von Karman, and compared with the experimental results. The timing and strain levels of the measured pulses are well duplicated by the calculation. However, the calculated pulses have much steeper fronts than are observed. For both rubber and nylon, in order to describe the impact response it is necessary to include a creep function as well as a dynamic stress-strain curve. So far it has not been possible to analyze a photograph of an impact on nylon yarn; this is because of large variations of strain with position.

UNCLASSIFIED

1. Stresses
2. Nylon
3. Rubber
4. Creep
5. Dynamics
6. Elasticity
7. Photographic analysis
8. Plasticity
9. Polymers
10. Stroboscopes
I. Title
II. Series
III. Pilsworth, Malcolm N., Jr.

AD- Div. 25, 14, 24 Accession No.

Quartermaster Research & Engineering Center, Natick, Mass.
TENSILE IMPACT ON RUBBER AND NYLON by Malcolm N. Pilsworth, Jr., 70 pp. illus. (Technical Report PR-3) May 1962

A method has been sought of describing the response of visco-elastic materials to loading when the velocity of strain propagation in the material is the controlling factor. A machine is described that delivers a longitudinal impact at about 150 ft/sec to a yarn or strip. The impact is photographed using a high-speed stroboscope and a moving mirror. Strain-time-position data are obtained from the picture. Results are given for the impact of a rubber strip. In another experimental technique the force at the fixed end of a nylon yarn during impact is measured. Tentative high-speed stress-strain curves were deduced, for the rubber from the photograph and for the nylon from another series of tests in which the acceleration of a tail mass was measured. Assuming that these curves hold during the impact with no time dependency, the strain patterns were computed by a method of

UNCLASSIFIED

1. Stresses
2. Nylon
3. Rubber
4. Creep
5. Dynamics
6. Elasticity
7. Photographic analysis
8. Plasticity
9. Polymers
10. Stroboscopes
I. Title
II. Series
III. Pilsworth, Malcolm N., Jr.

Quartermaster Research & Engineering Center, Natick, Mass.
TENSILE IMPACT ON RUBBER AND NYLON by Malcolm N. Pilsworth, Jr., 70 pp. illus. (Technical Report PR-3) May 1962

A method has been sought of describing the response of visco-elastic materials to loading when the velocity of strain propagation in the material is the controlling factor. A machine is described that delivers a longitudinal impact at about 150 ft/sec to a yarn or strip. The impact is photographed using a high-speed stroboscope and a moving mirror. Strain-time-position data are obtained from the picture. Results are given for the impact of a rubber strip. In another experimental technique the force at the fixed end of a nylon yarn during impact is measured. Tentative high-speed stress-strain curves were deduced, for the rubber from the photograph and for the nylon from another series of tests in which the acceleration of a tail mass was measured. Assuming that these curves hold during the impact with no time dependency, the strain patterns were computed by a method of characteristics given by von Karman, and compared with the experimental results. The timing and strain levels of the measured pulses are well duplicated by the calculation. However, the calculated pulses have much steeper fronts than are observed. For both rubber and nylon, in order to describe the impact response it is necessary to include a creep function as well as a dynamic stress-strain curve. So far it has not been possible to analyze a photograph of an impact on nylon yarn; this is because of large variations of strain with position.

1. Stresses
2. Nylon
3. Rubber
4. Creep
5. Dynamics
6. Elasticity
7. Photographic analysis
8. Plasticity
9. Polymers
10. Stroboscopes
I. Title
II. Series
III. Pilsworth, Malcolm N., Jr.

AD- Div. 25, 14, 24 Accession No.

Quartermaster Research & Engineering Center, Natick, Mass.
TENSILE IMPACT ON RUBBER AND NYLON by Malcolm N. Pilsworth, Jr., 70 pp. illus. (Technical Report PR-3) May 1962

A method has been sought of describing the response of visco-elastic materials to loading when the velocity of strain propagation in the material is the controlling factor. A machine is described that delivers a longitudinal impact at about 150 ft/sec to a yarn or strip. The impact is photographed using a high-speed stroboscope and a moving mirror. Strain-time-position data are obtained from the picture. Results are given for the impact of a rubber strip. In another experimental technique the force at the fixed end of a nylon yarn during impact is measured. Tentative high-speed stress-strain curves were deduced, for the rubber from the photograph and for the nylon from another series of tests in which the acceleration of a tail mass was measured. Assuming that these curves hold during the impact with no time dependency, the strain patterns were computed by a method of

UNCLASSIFIED

1. Stresses
2. Nylon
3. Rubber
4. Creep
5. Dynamics
6. Elasticity
7. Photographic analysis
8. Plasticity
9. Polymers
10. Stroboscopes
I. Title
II. Series
III. Pilsworth, Malcolm N., Jr.

Quartermaster Research & Engineering Center, Natick, Mass.
TENSILE IMPACT ON RUBBER AND NYLON by Malcolm N. Pilsworth, Jr., 70 pp. illus. (Technical Report PR-3) May 1962

A method has been sought of describing the response of visco-elastic materials to loading when the velocity of strain propagation in the material is the controlling factor. A machine is described that delivers a longitudinal impact at about 150 ft/sec to a yarn or strip. The impact is photographed using a high-speed stroboscope and a moving mirror. Strain-time-position data are obtained from the picture. Results are given for the impact of a rubber strip. In another experimental technique the force at the fixed end of a nylon yarn during impact is measured. Tentative high-speed stress-strain curves were deduced, for the rubber from the photograph and for the nylon from another series of tests in which the acceleration of a tail mass was measured. Assuming that these curves hold during the impact with no time dependency, the strain patterns were computed by a method of characteristics given by von Karman, and compared with the experimental results. The timing and strain levels of the measured pulses are well duplicated by the calculation. However, the calculated pulses have much steeper fronts than are observed. For both rubber and nylon, in order to describe the impact response it is necessary to include a creep function as well as a dynamic stress-strain curve. So far it has not been possible to analyze a photograph of an impact on nylon yarn; this is because of large variations of strain with position.

1. Stresses
2. Nylon
3. Rubber
4. Creep
5. Dynamics
6. Elasticity
7. Photographic analysis
8. Plasticity
9. Polymers
10. Stroboscope
I. Title
II. Series
III. Pilsworth, Malcolm N., Jr.

These variations may be errors introduced by the poorer quality of the photograph of nylon, but since the variations could not be removed by special smoothing techniques, the tentative conclusion is that they are real.

These variations may be errors introduced by the poorer quality of the photograph of nylon, but since the variations could not be removed by special smoothing techniques, the tentative conclusion is that they are real.

These variations may be errors introduced by the poorer quality of the photograph of nylon, but since the variations could not be removed by special smoothing techniques, the tentative conclusion is that they are real.

These variations may be errors introduced by the poorer quality of the photograph of nylon, but since the variations could not be removed by special smoothing techniques, the tentative conclusion is that they are real.

AD- Div. 25, 14, 24 Accession No.

Quartermaster Research & Engineering Center, Natick, Mass.
TENSILE IMPACT ON RUBBER AND NYLON by Malcolm N. Pilsworth, Jr., 70 pp, illus. (Technical Report PR-3) May 1962

A method has been sought of describing the response of visco-elastic materials to loading when the velocity of strain propagation in the material is the controlling factor. A machine is described that delivers a longitudinal impact at about 150 ft/sec to a yarn or strip. The impact is photographed using a high-speed stroboscope and a moving mirror. Strain-time-position data are obtained from the picture. Results are given for the impact of a rubber strip. In another experimental technique the force at the fixed end of a nylon yarn during impact is measured. Tentative high-speed stress-strain curves were deduced, for the rubber from the photograph and for the nylon from another series of tests in which the acceleration of a tail mass was measured. Assuming that these curves hold during the impact with no time dependency, the strain patterns were computed by a method of characteristics given by von Karman, and compared with the experimental results. The timing and strain levels of the measured pulses are well duplicated by the calculation. However, the calculated pulses have much steeper fronts than are observed. For both rubber and nylon, in order to describe the impact response it is necessary to include a creep function as well as a dynamic stress-strain curve. So far it has not been possible to analyze a photograph of an impact on nylon yarn; this is because of large variations of strain with position.

UNCLASSIFIED

1. Stresses
2. Nylon
3. Rubber
4. Creep
5. Dynamics
6. Elasticity
7. Photographic analysis
8. Plasticity
9. Polymers
10. Stroboscopes
I. Title
II. Series
III. Pilsworth, Malcolm N., Jr.

AD- Div. 25, 14, 24 Accession No.

Quartermaster Research & Engineering Center, Natick, Mass.
TENSILE IMPACT ON RUBBER AND NYLON by Malcolm N. Pilsworth, Jr., 70 pp, illus. (Technical Report PR-3) May 1962

A method has been sought of describing the response of visco-elastic materials to loading when the velocity of strain propagation in the material is the controlling factor. A machine is described that delivers a longitudinal impact at about 150 ft/sec to a yarn or strip. The impact is photographed using a high-speed stroboscope and a moving mirror. Strain-time-position data are obtained from the picture. Results are given for the impact of a rubber strip. In another experimental technique the force at the fixed end of a nylon yarn during impact is measured. Tentative high-speed stress-strain curves were deduced, for the rubber from the photograph and for the nylon from another series of tests in which the acceleration of a tail mass was measured. Assuming that these curves hold during the impact with no time dependency, the strain patterns were computed by a method of characteristics given by von Karman, and compared with the experimental results. The timing and strain levels of the measured pulses are well duplicated by the calculation. However, the calculated pulses have much steeper fronts than are observed. For both rubber and nylon, in order to describe the impact response it is necessary to include a creep function as well as a dynamic stress-strain curve. So far it has not been possible to analyze a photograph of an impact on nylon yarn; this is because of large variations of strain with position.

UNCLASSIFIED

1. Stresses
2. Nylon
3. Rubber
4. Creep
5. Dynamics
6. Elasticity
7. Photographic analysis
8. Plasticity
9. Polymers
10. Stroboscopes
I. Title
II. Series
III. Pilsworth, Malcolm N., Jr.

AD- Div. 25, 14, 24 Accession No.

Quartermaster Research & Engineering Center, Natick, Mass.
TENSILE IMPACT ON RUBBER AND NYLON by Malcolm N. Pilsworth, Jr., 70 pp, illus. (Technical Report PR-3) May 1962

A method has been sought of describing the response of visco-elastic materials to loading when the velocity of strain propagation in

UNCLASSIFIED

1. Stresses
2. Nylon
3. Rubber
4. Creep
5. Dynamics

AD- Div. 25, 14, 24 Accession No.

Quartermaster Research & Engineering Center, Natick, Mass.
TENSILE IMPACT ON RUBBER AND NYLON by Malcolm N. Pilsworth, Jr., 70 pp, illus. (Technical Report PR-3) May 1962

A method has been sought of describing the response of visco-elastic materials to loading when the velocity of strain propagation in

UNCLASSIFIED

1. Stresses
2. Nylon
3. Rubber
4. Creep
5. Dynamics

AD- Div. 25, 14, 24 Accession No.

Quartermaster Research & Engineering Center, Natick, Mass.
TENSILE IMPACT ON RUBBER AND NYLON by Malcolm N. Pilsworth, Jr., 70 pp. illus. (Technical Report PR-8) May 1962

A method has been sought of describing the response of viscoelastic materials to loading when the velocity of strain propagation in the material is the controlling factor. A machine is described that delivers a longitudinal impact at about 150 ft/sec to a yarn or strip. The impact is photographed using a high-speed stroboscope and a moving mirror. Strain-time-position data are obtained from the picture. Results are given for the impact of a rubber strip. In another experimental technique the force at the fixed end of a nylon yarn during impact is measured. Tentative high-speed stress-strain curves were deduced, for the rubber from the photograph and for the nylon from another series of tests in which the acceleration of a tail mass was measured. Assuming that these curves hold during the impact with no time dependency, the strain patterns were computed by a method of characteristics given by von Karman, and compared with the experimental results. The timing and strain levels of the measured pulses are well duplicated by the calculation. However, the calculated pulses have much steeper fronts than are observed. For both rubber and nylon, in order to describe the impact response it is necessary to include a creep function as well as a dynamic stress-strain curve. So far it has not been possible to analyze a photograph of an impact on nylon yarn, this is because of large variations of strain with position.

UNCLASSIFIED

1. Stresses
2. Nylon
3. Rubber
4. Creep
5. Dynamics
6. Elasticity
7. Photographic analysis
8. Plasticity
9. Polymers
10. Stroboscopes
I. Title
II. Series
III. Pilsworth, Malcolm N., Jr.

AD- Div. 25, 14, 24 Accession No.

Quartermaster Research & Engineering Center, Natick, Mass.
TENSILE IMPACT ON RUBBER AND NYLON by Malcolm N. Pilsworth, Jr., 70 pp. illus. (Technical Report PR-8) May 1962

A method has been sought of describing the response of viscoelastic materials to loading when the velocity of strain propagation in the material is the controlling factor. A machine is described that delivers a longitudinal impact at about 150 ft/sec to a yarn or strip. The impact is photographed using a high-speed stroboscope and a moving mirror. Strain-time-position data are obtained from the picture. Results are given for the impact of a rubber strip. In another experimental technique the force at the fixed end of a nylon yarn during impact is measured. Tentative high-speed stress-strain curves were deduced, for the rubber from the photograph and for the nylon from another series of tests in which the acceleration of a tail mass was measured. Assuming that these curves hold during the impact with no time dependency, the strain patterns were computed by a method of characteristics given by von Karman, and compared with the experimental results. The timing and strain levels of the measured pulses are well duplicated by the calculation. However, the calculated pulses have much steeper fronts than are observed. For both rubber and nylon, in order to describe the impact response it is necessary to include a creep function as well as a dynamic stress-strain curve. So far it has not been possible to analyze a photograph of an impact on nylon yarn, this is because of large variations of strain with position.

UNCLASSIFIED

1. Stresses
2. Nylon
3. Rubber
4. Creep
5. Dynamics
6. Elasticity
7. Photographic analysis
8. Plasticity
9. Polymers
10. Stroboscopes
I. Title
II. Series
III. Pilsworth, Malcolm N., Jr.

These variations may be errors introduced by the poorer quality of the photograph of nylon, but since the variations could not be removed by special smoothing techniques, the tentative conclusion is that they are real.

These variations may be errors introduced by the poorer quality of the photograph of nylon, but since the variations could not be removed by special smoothing techniques, the tentative conclusion is that they are real.

These variations may be errors introduced by the poorer quality of the photograph of nylon, but since the variations could not be removed by special smoothing techniques, the tentative conclusion is that they are real.

These variations may be errors introduced by the poorer quality of the photograph of nylon, but since the variations could not be removed by special smoothing techniques, the tentative conclusion is that they are real.

HEADQUARTERS
QUARTERMASTER RESEARCH & ENGINEERING COMMAND, US ARMY
Quartermaster Research & Engineering Center
Natick, Massachusetts

PIONEERING RESEARCH DIVISION

Technical Report
PR-3

TENSILE IMPACT ON RUBBER AND NYLON

Malcolm N. Pilsworth, Jr.
Thermodynamics Laboratory

Project Reference:
7X 99-25-001

May 1962

FOREWORD

Several years ago a program was initiated in the Pioneering Research Division for the study of the properties of materials at high rates of strain. An examination of the literature on the subject indicated that the most likely area for new and interesting results was where the disturbance in the material proceeds in waves even though the loading, after an initial impact, is steady. This is caused by the limited velocity of propagation of a disturbance in any material (similar to the velocity of sound). This condition may be most easily realized and understood with tensile impact on visco-elastic materials. This report describes the experimental procedure and discusses the information obtained so far concerning the nature of the strain waves.

S. DAVID BAILEY, Ph. D.
Chief
Pioneering Research Division

Approved:

DALE H. SIELING, Ph. D.
Scientific Director
QM Research and Engineering Command

MERRILL L. TRIBE
Brigadier General, USA
Commanding
QM Research and Engineering Command

CONTENTS

ABSTRACT

A method has been sought of describing the response of visco-elastic materials to loading when the velocity of strain propagation in the material is the controlling factor. A machine is described that delivers a longitudinal impact at about 150 ft/sec to a yarn or strip. The impact is photographed using a high-speed stroboscope and a moving mirror. Strain-time-position data are obtained from the picture. Results are given for the impact of a rubber strip. In another experimental technique the force at the fixed end of a nylon yarn during impact is measured. Tentative high-speed stress-strain curves were deduced, for the rubber from the photograph and for the nylon from another series of tests in which the acceleration of a tail mass was measured. Assuming that these curves hold during the impact with no time dependency, the strain patterns were computed by a method of characteristics given by von Karman, and compared with the experimental results. The timing and strain levels of the measured pulses are well duplicated by the calculation. However, the calculated pulses have much steeper fronts than are observed. For both rubber and nylon, in order to describe the impact response it is necessary to include a creep function as well as a dynamic stress-strain curve. So far it has not been possible to analyze a photograph of an impact on nylon yarn; this is because of large variations of strain with position. These variations may be errors introduced by the poorer quality of the photograph of nylon, but since the variations could not be removed by special smoothing techniques, the tentative conclusion is that they are real.

TENSILE IMPACT ON RUBBER AND NYLON

PART I. PROBLEM, PROCEDURES AND METHODS

1. Introduction

The visco-elastic properties of polymeric materials have been under investigation for many years. Much of the behavior of nylon and rubber, the materials investigated in the present study, is well understood. Until recently, however, only a limited amount of work has been done in which the material is strained rapidly.

When the rate of strain is sufficiently rapid, the waves or pulses that distribute the strain are no longer of very small amplitude, and it is no longer proper to assume that the strain is uniform throughout the sample. At slow rates of strain the momentum imparted to various parts of the sample by the applied stress is negligible and the role of inertial forces is very small. But at high rates of strain inertial forces become very large. A tensile stress, if applied to a string with sufficient rapidity, will cause the string to break without the transmission of any stress to the remote end of the string. The string is simply torn in two by the applied force and the opposing force of inertia.

In the study of the response of polymers to stress, the principle of the equivalence of time and temperature has been surprisingly useful. This principle permits (for example) creep curves obtained at widely different temperatures to be pieced together into a single master curve of strain as a function of the logarithm of the time. From such a master curve, the response of a material occurring in the first few milliseconds after application of a stress can be inferred from experimental data taken over a much longer time, but at a lower temperature.

But predictions of short-time behavior based on the principle of the equivalence of time and temperature can be accepted only

provisionally, and must as far as possible be validated by direct experiments in which stresses are applied in the shortest practical time interval.

In our experiments the strain rates have been high enough to produce strain waves that are easily observable. The sample is in the form of a string, which is stretched by setting one end in motion with a velocity of about 160 feet per second. The strain pulse generated by the impact travels back and forth along the string three or four times in a typical experiment, and the string usually breaks as the pulse begins its fourth or fifth passage.

The time of one of our experiments from impact to break is approximately 10 millisec for rubber and 2 millisec for nylon. These times are very short compared to the time required to obtain a stress-strain curve, with, for example, an Instron tensile tester. They are somewhat longer than the time required for a shell fragment to penetrate a layer of nylon body armor. (Responses occurring in very much shorter times ($\sim$ 1 microsec) may be studied by subjecting materials to ultrasonic vibrations. This technique has the limitation, however, that the strains produced are small compared to the breaking strain.)

The results presented here give information on the shapes of the strain pulses and their velocity. It is shown that stress-strain curves alone are insufficient to explain the behavior of the strain pulses. Even in times of a few milliseconds an appreciable amount of creep occurs.

2. Related Studies

There has been little work reported about the longitudinal impact on flexible polymeric materials. Schiefer, Smith, et al. [1-3],* worked at impact velocities in this region and measured various quantities including over-all strain, but did not directly observe strain as a function of position on the string. They also worked with transverse impact where there is a transverse wave

* Figures in brackets indicate references, listed at end of this report.

of motion and a longitudinal strain wave. Stewart, et al., also reported on transverse impact and measured the strain as a function of position on the string [4, 5]. Brinkworth [6] reported on studies of the first pulse when a long cable was impacted longitudinally.

There has been considerable work done on impact below the speeds where wave motion predominates [7] and some work done at high speeds but with short samples so that many reflections occur [8].

The theoretical groundwork for much of the analysis is given by von Karman [9-11]. He assumed the material was obeying a fixed stress-strain curve and developed the equations accordingly.

The validity of von Karman's analysis does not depend on the nature of the material, except in the question of the validity of the assumption of a fixed stress-strain curve. Though not explicitly stated, he was apparently considering metals where this assumption may be reasonably valid for many purposes. However, it is not valid for visco-elastic materials where there may be appreciable creep present. Nevertheless it is convenient to use von Karman's analysis as a starting point, and to supplement it by corrections that take creep into account.

3. Stress-strain curves and creep curves

When a material is stressed it changes configuration or, in other words, exhibits strain. This change requires time. In a particular event, if the time is not sufficient the change will not be complete. Therefore any stress-strain curve, other than an equilibrium stress-strain curve, should be marked as to the rate at which it was measured or for which it is applicable. The more rapidly a material responds, the higher the rate has to be before the stress-strain curve is appreciably different from a slow-speed or equilibrium curve.

If a material could be uniformly stressed at a high speed, a stress-strain curve corresponding to this speed would completely

define its response. On the other hand, if the stress at a particular location in the material were constant for a length of time, the strain would vary according to a creep curve. If we had a complete family of creep curves at different stresses the response of the material to a uniform stress at any speed would be defined. The stress-strain curve corresponding to any stress-time curve could be determined directly.

Although most stresses may not be applied uniformly, with simple geometry and slow speeds the stress will equalize throughout the sample. An example of this is the tension test made with an Instron machine. In a tensile impact experiment, which is only a tension test at very high speed, we must consider the velocity with which a disturbance may travel in the material in order to bring about the equalization. If the strain wave velocity is low enough and the impact velocity high enough, the disturbance will travel along the sample as a strain wave or pulse with an amplitude that is an appreciable fraction of the breaking strain. In this case the stress at any position along the sample is changing very rapidly when the wave reaches that point and may be constant for a time after it passes. So not having a fixed rate at which the stress is increasing, we cannot, theoretically at least, determine a fixed stress-strain curve that will apply to the experiment, either from a family of creep curves or any other way.

However, if we assume that we can use a fixed stress-strain curve for a particular experiment, we can derive equations and use procedures that will show what the strain wave pattern would be in the absence of creep. The equations and procedures will be discussed later. The time involved in an impact experiment is of course very short and the creep occurring in this time may be very small. If this creep were small enough compared to other strains involved, it could be ignored. If so, a fixed stress-strain curve could be used and a good picture of the response of the material could be obtained from the equations and procedures mentioned above. Or if the creep is not small enough to be completely ignored, it still may be small enough so as to not affect the shape of the stress-strain curve appreciably. In this case the equations and procedures that assume a fixed stress-strain curve can be used

to obtain a strain wave pattern and the creep added to this to get a complete picture.

4. Strain waves ignoring creep

We will now develop the equations for the strain waves resulting from tensile impact without considering creep.

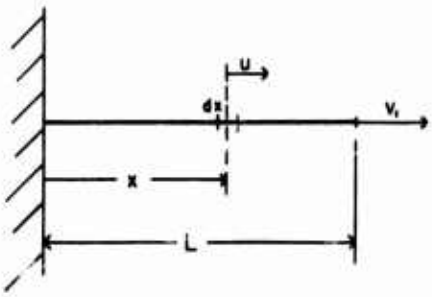

Figure 1. Diagram of tensile impact.

Consider a string of length L (Figure 1) fastened at one end and suddenly set into motion at the other with a velocity v_1. Let x be position on the sample. Strictly speaking x is not a distance or a length but is numerically equal to distance or length on the original unstrained sample. We may now consider displacement (u), strain (ϵ), stress (σ), particle velocity (v) and propagation velocity (c) as functions of position (x) and time (t) with much simpler equations and graphical representations than if x were distance. These are called Lagrangian coordinates.

The stress (σ) is defined as "the ratio of the tension between two portions of the sample to the initial cross-sectional area of the sample." This definition is used since it fits into the equation of motion with Lagrangian coordinates. It is also the definition easiest to use for slow-speed stress-strain curves, since the values may be obtained without measurement of strained cross-sectional areas or knowledge of Poisson's ratio.

Let u be the displacement of an element. It is the distance that an element at a position x will have moved at time t and so is a function of both x and t. The actual physical velocity of the element is $v = \partial u/\partial t$. When x equals L, v equals v_1.

If the displacement at one end of an element dx is u, that at the other end is $u + \partial u/\partial x\, dx$ and the elongation is $u + \partial u/\partial x$

dx - u. Since x is numerically equal to distance on the unstrained sample, the strain is

$$\epsilon = \frac{\partial u/\partial x \, dx}{dx} = \frac{\partial u}{\partial x} .$$

If the force on one end of an element dx is σ A, that at the other end is σ A + $\partial\sigma/\partial x$ dx A and the net force is $\partial\sigma/\partial x$ dx A. From our definition of σ we see that A here must be original cross-sectional area. The mass on which this acts is ρAdx with A as above and ρ the original density. The fact that we have not used true stresses or actual cross sections does not matter since the relations above give the force on, and mass of, an element dx.

Acceleration is $\partial^2u/\partial t^2$ whence the equation of motion of an element is $\partial\sigma/\partial x$ dxA = ρdxA $\partial^2u/\partial t^2$. Or cancelling out:

$$\frac{\partial\sigma}{\partial x} = \rho \frac{\partial^2 u}{\partial t^2} .$$

We now assume that stress is a function of strain only and not of time, $\sigma = f(\epsilon)$. Strictly this means that there is only one stress-strain curve, static or dynamic. But we may take it to mean that any change in the stress-strain relation for the duration of the motion to be considered is not appreciable or, in other words, we ignore any creep that may occur. This allows the use of dynamic stress-strain relations.

Then we may write $\partial\sigma/\partial x = d\sigma/d\epsilon \; \partial\epsilon/\partial x$, and since $\epsilon = \partial u/\partial x$, then $\partial\epsilon/\partial x = \partial^2u/\partial x^2$. Hence we have $d\sigma/d\epsilon \; \partial^2u/\partial x^2 = \rho \; \partial^2u/\partial t^2$. This is a wave equation, the general form of which is $c^2 \; \partial^2u/\partial x^2 = \partial^2u \; \partial t^2$. So we have

$$c = \sqrt{1/\rho \; d\sigma/d\epsilon}$$

where c is the rate of propagation of a disturbance in the (x, t) plane. If u were transverse or some other form of displacement so that x was always numerically equal to distance, c would be the actual physical velocity of the disturbance in laborator,

coordinates. Since u is in the same direction as x, this is not so and at large strains the velocity in laboratory coordinates would be much greater than c. The quantity c is a function of strain and for a particular ϵ is given by the slope of the stress-strain curve as in the equation derived above. Also, c is equal to the slope of a line of constant strain drawn in the (x, t) plane.

For tensile impact within the elastic limit $d\sigma/d\epsilon = E$ (Young's Modulus) so

$$c = c_0 = \sqrt{E/\rho}\,.$$

This is a constant velocity of propagation and in any material c_0 is the velocity of the leading edge of a longitudinal strain. In an ideal impact the end of the sample will start to move at time zero with a velocity v_1, and continue at this velocity. In an elastic material at time t the disturbance will have traveled a distance c_0t, so this will be the length of the original material affected up to this time. The end will have moved a distance v_1t, the new length of the affected material will be $c_0t + v_1t$, the elongation will be v_1t, and the strain will be $v_1t/c_0t = v_1/c_0$. Thus the strain is not a function of time, at least not a continuous function. If we measure x from the fixed end and call the total length L, for $x < (L - c_0t)$ the strain is zero and for $x > (L - c_0t)$ the strain is v_1/c_0. Thus we have a square wave front. It reflects at the fixed end and continues back and forth, increasing by v_1/c_0 at each reflection until failure.

If the material is not elastic but still obeys a relation $\sigma = f(\epsilon)$ there is still a discrete pulse. Its height was shown by von Karman [9-11] to be given by the relation

$$v_1 = \int_0^{\epsilon_1} c\,d\epsilon$$

where v_1 is the impact velocity,
ϵ_1 is the height of the strain pulse, and
$c = \sqrt{1/\rho\ d\sigma/d\epsilon}$ and so is a function of ϵ.

The front of the pulse is not square or of any constant shape since

each increment of strain travels at a different velocity. The reflections will not be simple but may be worked out by a method of characteristics using $v \pm \int c\,d\epsilon$ = constants as the characteristics. More details of this will be given when the analyses carried out are discussed.

5. Purpose and procedure

When a material, particularly a visco-elastic material, is impacted in such a way that the velocity of propagation of a disturbance in the material is a dominating property, how may we observe the response and also how may we describe or characterize the response? These are the questions for which we are seeking answers.

Since the degree of stress and strain is not uniform along the sample, observations must be made that include the whole sample. Photography seems to be called for here. The method of using a stroboscope, moving mirror, and still camera was chosen since it seemed to be most adaptable to the already-constructed impact apparatus. Details, results, and proposed improvements will be discussed below.

Stress or force can probably be measured only at the ends of the sample. Since a direct measurement of force has not yet been made in the present work, the reasons for not doing so should be given. The principal difficulty is the rapidity of response of the force-measuring device. Although the force probably does not change as rapidly as the simple picture discussed in the previous section would indicate, rise times calculated from such considerations are conceivable and for reliable results we must be sure that we are not limited by the limitations of the measuring instrument. Piezoelectric force gages seem to be the best of the commercially-available devices. Their high-frequency response depends on their having a small mass and any increase in this mass due to jaws or other mounting devices seriously affects them. Semiconductor strain gages, being developed at several laboratories, seem to offer possibilities.

Three indirect methods for determining stress have been used in the present work. One method was to calculate σ from measured and deduced values of the propagation velocity, c. Both the other methods required special experimental setups. In one the fixed support was replaced by a tail mass, the motion of this tail mass observed, and its acceleration calculated. The other used a calibrated weak link in place of the fixed support. These will all be discussed below.

To our knowledge there has been no analytical solution to the problem of impact on nonlinear visco-elastic materials. Von Karman's solution is for nonlinear rate-independent materials. Most of the analytical work on visco-elastic materials is for linear materials. (A linear visco-elastic material is one that can be represented by a combination of Hookean springs in which the stress is proportional to the strain, and Newtonian dash pots in which the stress is proportional to the strain rate. Real materials are linear only for small strains.)

We are not seeking an analytical solution at this time but rather a means of describing the response that would enable us to predict what would happen with samples of other lengths and at other velocities of impact. If such a description can be reduced to simple enough parameters, it will provide the necessary starting point for the analytical solution of nonlinear visco-elastic impact. Also, this description, with or without the analytical solution, will be helpful, or perhaps even necessary, in determining the molecular mechanisms involved in this type of straining.

There are two general areas that may be covered in a description of the response. One is the response occurring as a pulse or wave motion and the other is a delayed response. Any division between these two types is arbitrary. In fact, the entire response could be thought of as in waves of very long length with trailing ends extending in time for the duration of the event. Some such consideration may lead to the analytical solution.

For the wave response we require a knowledge of the variations in the propagation velocity. The assumption that part of the response may be expressed as a dynamic stress-strain curve limits these variations to those consistent with the slope of the stress-strain curve and introduces a division between wave and delayed response.

The delayed response is called "creep," partly for want of a better word and partly because some work has been done on rubber to show that creep is continuous from times much shorter than those encountered here to the long times usually involved in creep measurements [12, 13]. This is discussed further in Part II below.

If we decide on the use of a stress-strain curve, as we have, we automatically separate the wave and delayed responses. The important question then is the relative magnitude of these responses. (Although we have been using the expression "delayed response," we must remember that the entire event takes only a few milliseconds and by "delayed" we mean that this part of the response does not occur in the fraction of a millisecond taken up by the passage of the wave front.) The creep curves for rubber given in references [12] and [13] indicate that, for rubber at least, the delayed response is appreciable.

Although it may not be possible to prove it, one can convince himself by repeated trials that when any conceivable stress-strain curve is selected to represent the entire response of a material, the resulting waves will be well-defined throughout the event. Therefore, if the experimentally observed waves are not well-defined, it means that the delayed response is appreciable. A measure of the relative magnitude of the responses may be made by finding a stress-strain curve that, when applied to the conditions of the test, reproduces the experimental strain levels. However, this strain will proceed in well-defined waves and we must then find the proper amount of creep or delayed response to smooth out the waves to the observed degree of definition.

In general, then, the procedure was to:

1. Impact the sample and measure in some way the strain wave pattern or some consequence of it.

2. Choose or determine a stress-strain curve.

3. Assuming that this curve represented the entire response, construct the response pattern for comparison with the measured pattern.

4. Add to this construction a delayed response, to see if the agreement between constructed and measured response could be improved.

6. Apparatus and testing procedure

A sling shot machine (see schematic diagram, Figure .) was constructed that used heavy rubber bands about 1/2 inch in cross section and 1 foot in diameter to accelerate a slider along a pair

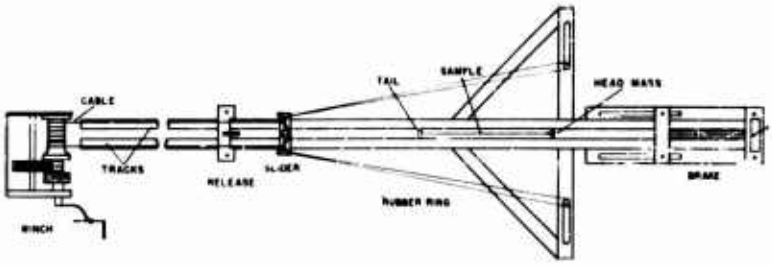

Figure 2. Rapid-impact machine.

of tracks. It was used routinely at slider velocities of about 130 feet per second (200 feet per second should be attainable). The

top velocity is probably limited by the retraction rate of the rubber. Another consideration at the higher speeds: it is difficult to stop the slider without damaging it. It is stopped with a spring-loaded brake that presses a brake band against the slider. The slider is made of steel and aluminum and weighs about 2 pounds.

The sample is placed between the tracks and is supported in various ways depending on the nature of the test. A T-shaped head mass is fastened to the front end of the string and the other end may be fixed solidly, fastened to a "weak link," fastened to a tail mass, or it could be connected to a force gage. Two projections on the bottom of the slider extend down between the tracks, straddle the tail support and sample and strike the arms of the head mass. After the impact the head mass accelerates very rapidly and goes ahead at a velocity somewhat greater than that of the slider, eventually passing completely through the tracks and being caught in a box.

The head mass is made of aluminum with pads of flocked nylon at the points where it is struck. In some forms it has means for guiding it to prevent it from hitting the sides of the track during the critical period. In the center of the head mass there is a hole tapered from front to back. There are wooden pins cut to fit this taper. The pins are sawed lengthwise along a wavy line. The sample is run through the hole, placed between the parts of the pin, and then the pin is driven into the hole.

Methods of taking data:

For complete information about an impact test we would like to know the value of the stress and the strain at all points in the sample at all times during the test. Obviously the stress or force cannot be measured directly within the material but only at the ends. The over-all strain or elongation of the entire sample may be easily determined but the local strain, $\partial u/\partial x$, is more difficult to measure. In an experiment of this nature, data may be taken in a variety of ways. In the first ("tail mass") method used here, the time for a tail mass at the end of the string to move a given distance was measured. A different kind of information was given

by the "weak link" method. With this, the end of the string was held by a "weak link" of known strength and the time after impact at which the link broke was measured. For measuring strain as a function of position on the string and of time, a high-speed stroboscope was used to take pictures.

In the tail mass method a tail mass, considerably lighter than the head mass, was fastened at the end of the string. Means were provided for placing fine copper wires across the path of the head and tail mass and the time between the breaking of two wires observed.

The times were at first measured with specially-built R-C decay circuits and an electrometer voltmeter, but in later experiments counter chronographs were available. Since only two times could be observed for each shot, it was necessary that many shots be made to get the complete time-distance curve of both masses. Since there was variation between shots even though the settings were maintained, one of the two times measured for each shot was used to determine the initial velocity of the head mass so that all shots could be corrected to an average head-mass velocity. One shot, for example, might have a wire just in front of the head mass and another wire 2 inches in front of the tail mass. The time determined from these two wires would be corrected according to the velocity of the head mass determined from two other wires.

The composite time-distance curves for the head and tail masses compiled in this way could be used to determine an overall strain-time curve. Also, by twice differentiating the curve for the tail mass, the curve for the force at the tail end could be determined. *

In the "weak link" method the tail of the string was fastened to a fixed support by a weak link composed of one or more strands

* The significance of the tail mass measurement was studied by Schiefer, Smith, et al. Parts I, II, and III of references [1, 2] and A. S. T. M. Bulletin 220 [3].

of fine copper wire. The time between impact, which broke a wire at the head mass, and the break of the link holding the tail was measured. The force required was assumed to be proportional to the number of strands. So a curve of the force at the tail versus time after impact could be built up this way.

Photographic method of measuring strain:

The most natural way to measure the local strain is photographic. A high-speed flash system was decided on rather than a framing camera or other device, and an Edgerton, Germeshausen and Grier No. 501 high-speed Stroboscope was obtained. This is rated to give 6000 flashes per second and can be used to 8000 per second or higher. A spring-loaded mirror was used to move the image across the film. A framework was built to support the light source, mirror, camera and shields above the tracks (see Figure 3).

There was some difficulty in illuminating the entire field enough for good photography with the stroboscope. For the pictures taken to date only about half the field was covered by the stroboscope and the rest with steady light. The sample was marked with regularly-spaced, contrasting marks that appeared as discrete marks under the strobe but as streaks under the steady light. The motion of the mirror introduced a regular distortion; therefore accurately-spaced, fixed markers were placed in the field for calibration. To date all pictures have been taken with a Polaroid camera with Polaroid 3000 speed film, 2 1/4 × 3 1/4, at lens speeds from f/4.5 to f/11. Although interesting and useful pictures have been obtained, we can expect better results with an improvement of illumination and optics.

The mirror has to move 18° to sweep the image from one side of the film to the other. The total swing of the mirror is about 30° and, in some cases, has to take place in about 5 millisec. A plate-glass mirror was tried and would not stand the shock with the present arrangement, so a polished steel mirror with a deposited chromium coating was used. Synchronization of the mirror is important. The mirror is released by a solenoid that is actuated

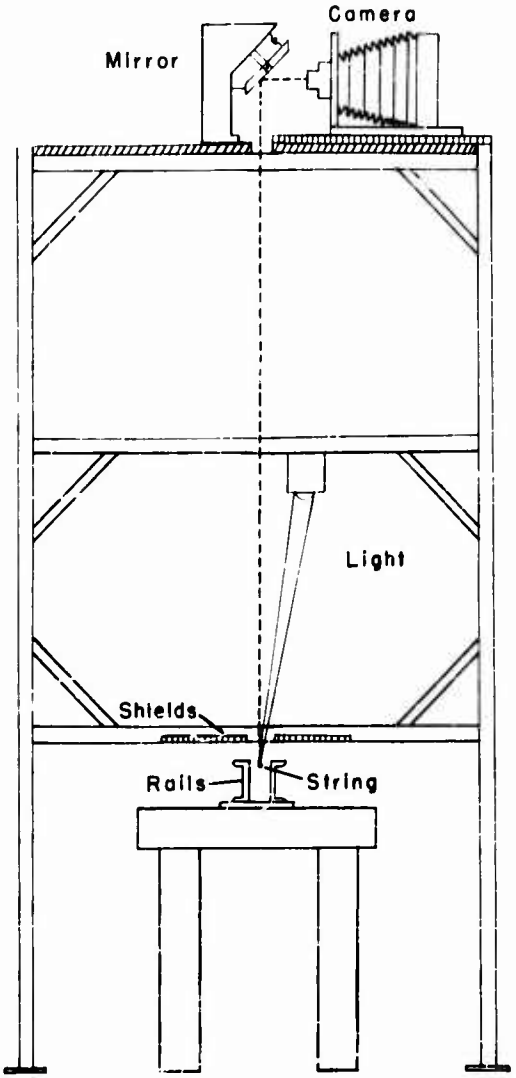

Figure 3. Apparatus for photographing rapid impact.

by the slider. There was some difficulty in getting a solenoid that would respond fast enough. A heavy keying relay that was constructed like a solenoid was found that could be made to work. In order to further increase its speed, it was safely overvolted by dumping the load of a large capacitor charged to the overvoltage into the solenoid. Though fast enough, the mirror release is still not very regular and it is necessary to take several pictures to learn the best setting and perhaps several more to get a perfectly synchronized picture.

7. Materials tested

Since the emphasis in the phase of the work reported here is on method of test and analysis and general nature of the response, the exact specification of the material is not of great importance. Probably the most important consideration is how well the material will photograph. It should have the proper surface and be of a color so that contrasting marks may be conveniently made on it.

The rubber used is particularly good in this respect. It is white, has a comparatively large cross section, exhibits large strains and has a low propagation velocity. A difficulty with the rubber was that in order to have the marks give good contrast when it was strained, the marks had to be made when it was strained. This procedure gave the rubber a slight set and would be an undesirable experimental condition for a study of the exact properties of the material. Also, it was difficult to clamp the rubber.

The rubber was designated by its supplier* as No. 12 nylon-white rubber. It has an 0.080 inch square cross section and is white. Our analytical laboratory determined that it contained 21% inorganic filler, presumably titanium dioxide.

The nylon yarn used is the same material used by the Textiles Section of NBS and by the Army Chemical Center in similar

* The Carr-Fulflex Company of Bristol, R. I.

tests [1-5]. It is the material used for weaving body armor, panels of which have been extensively tested in the Ballistics range at this Center. It is specified as high-tenacity nylon yarn, duPont type 300, 5 ply, 210 denier per ply, 3Z twist, 1066 denier total.

Since the nylon yarn presents a much smaller surface to the camera than the rubber and undergoes much smaller strains, it is more difficult to get good pictures and accurate data with it. Since it is very white and marks easily it is probably a better photographic subject than most yarns or filaments. However, the very fiber construction that makes it so white makes it difficult to have a sharp line between the marked and unmarked portions; this is necessary for precision measurements. Also, a yarn may not be the best material for basic studies in this field since the structure of the yarn may be fully as important as the structure of the polymer.

When the experimental technique is perfected and the description of response is reduced to variables that may be compared with measurements made in other ways, it would be better to work with controlled materials such as special nylon samples, pure gum rubber with specified vulcanization, or NBS isobutylene.

PART II. RUBBER STRIP

When measurements were first made with the rapid impact machine, it had not been decided what photographic technique to use, if any. The measurements were made principally on the nylon yarn using the tail mass and weak link methods. When the stroboscope was obtained, it was decided to start using it with a material that would photograph easily and have large, easily-measured strains. The choice was rubber. The photographic data for rubber are those for which the most complete analysis of strain waves is possible and so rubber is discussed first. Since rubber was chosen for its adaptability to the photographic method, the tail mass and weak link methods were not used with rubber.

1. Impact data

The best picture of rubber impact obtained and the one from which all the data for rubber were taken is shown in Figure 4. The narrow white lines on either side of the picture are the calibration marks, 100 cm between inside edges. At the very top of the picture may be seen the undisturbed sample attached to the head mass; in this case the head mass has a long extension on it so that it is as long as the sample. Without this extension, a large part of the sample would have been hidden by the slider as impact occurred. A portion of the slider is then seen passing over the sample and hitting the head mass; the head mass goes a little ahead of the slider and is identified by the small white square on it. The head mass and slider soon pass out of the strobe region into the steady-light region where they make streaks. In the meantime, the increase of strain in the sample may be observed and its wave nature is apparent. Only a small portion of the sample passed out of the strobe region. In successive tests the sample may fail at the head, the tail, or both. This one failed at the head and the very rapid retraction of the rubber may be observed. The end moved at about 16 cm per millisec or 525 feet per second.

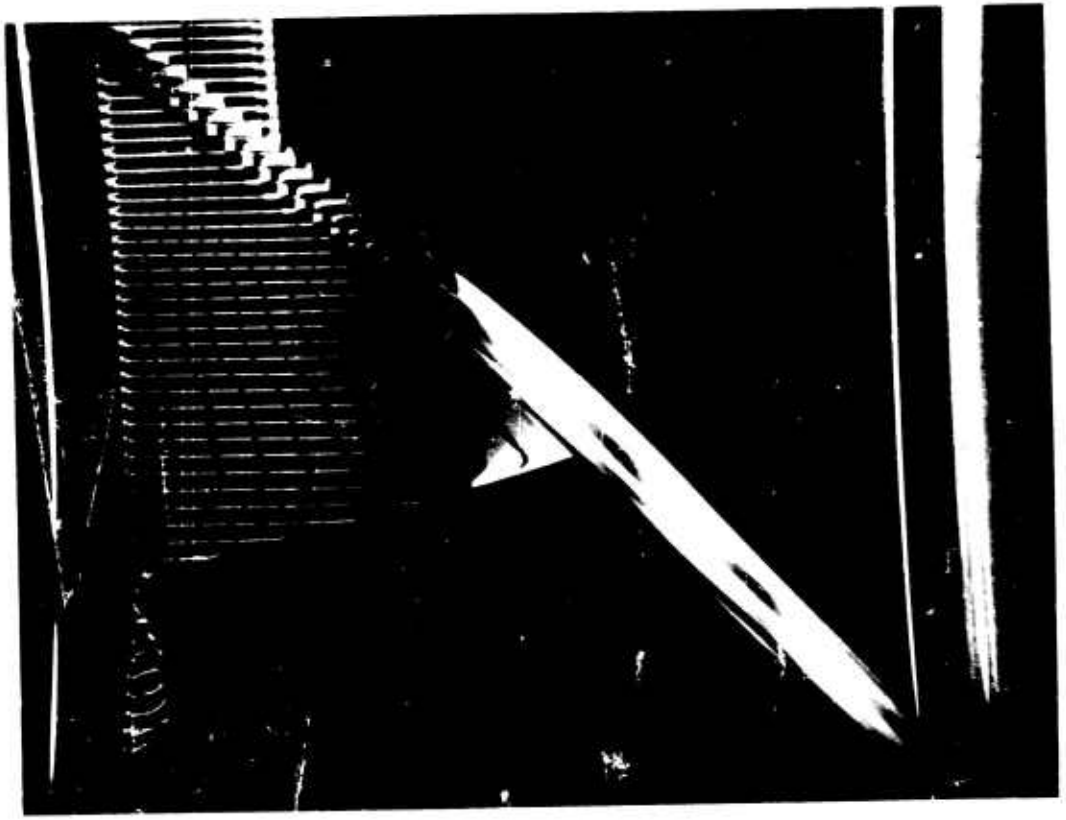

Figure 4. Rubber impacted at 138 ft/sec. 10-cm sample. Strobe rate 2000/sec. f/11 on Polaroid 3000.

The sample was 10 cm long and marked at every centimeter. The velocity of the head mass was 4.2 cm per millisec or 138 feet per second. The picture was taken at a stroboscope frequency of 2000 per second and at f/11 on Polaroid 3000 film.

The picture was measured with a measuring microscope. For each flash the position of each mark was measured as well as the position of the calibration marks. From the known separation of the calibration marks a factor was determined to correct the measured positions of the marks. An undistorted picture could then be drawn of the motion of each mark (Figure 5). The sample broke at the head 10.5 millisec after impact at a total length of 53 cm or 5.3 times its original length.

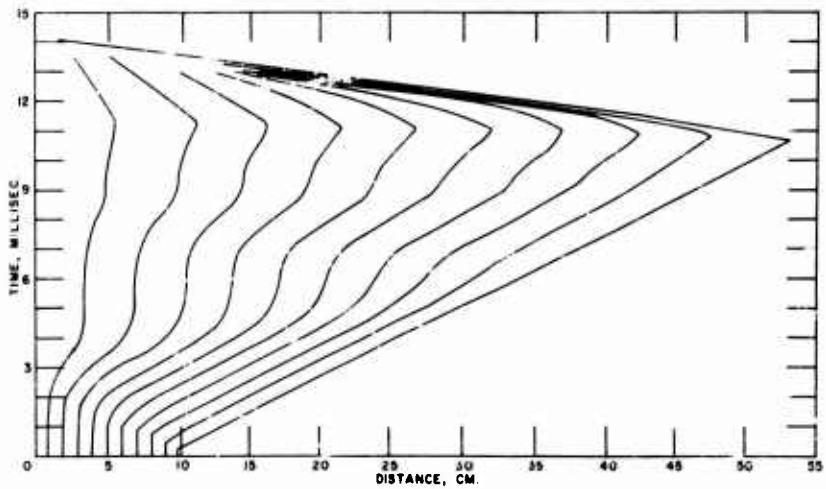

Figure 5. From Figure 4: Distortion corrected and motion of each mark shown.

From the corrected position data the strain for each centimeter interval and at every 0.5 millisec (every flash) was calculated. The strain is then plotted against position on the sample

for each time interval. The position coordinate used is position on the original or unstrained sample. The strain is given as a strain ratio rather than a percentage. Thus a strain of 1.00 would mean the original length was doubled. Strain profiles plotted in this way required some smoothing but not very much. This is shown in Figure 6 where the data and smooth curves for a few of the times are plotted. In the space-time regions where the strain seemed to remain constant for a few milliseconds the data were most erratic and the values in those regions were averaged and straight lines drawn. These were at strains of 1.28 near the head and 2.53 at the tail.

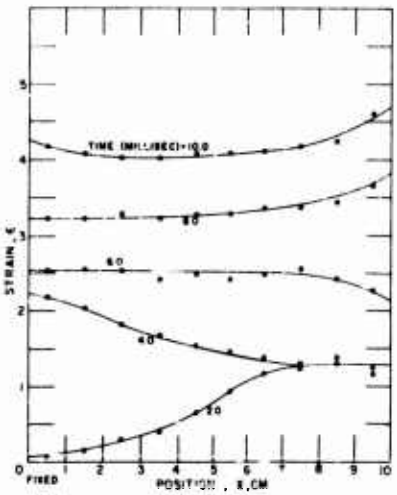

Figure 6. Rubber impact. Strain vs. position for several times, showing data and extent of smoothing required.

The smoothed plot of strain against position for fixed times is shown (Figure 7). The theoretical constructions with which we are to compare the data will be made with position and time as coordinates. Hence it is useful to present the information contained in Figure 7 in a different way, interchanging the roles of the ordinate (strain) and the parameter (time).

The resulting graph is shown in Figure 8. In both the (x, ϵ) (Figure 7) and the (x, t) (Figure 8) diagrams the wave nature of the response is very evident at first but after a single reflection the picture is more confused.

In studying Figure 8 one may note that the line for zero strain has some curvature. If, as has been stated, c_0 is the velocity of propagation of the initial disturbance in any material and is a constant equal to $\sqrt{E/\rho}$, shouldn't this line be straight? One can think of a number of reasons why the experimentally-determined line is not straight but the most likely seems to be that it is not really a line of zero strain. It is a line just below that for the smallest detectable strain. If this smallest detectable strain is above the elastic limit, which is very low for rubber, there is no reason for the line to be exactly straight.

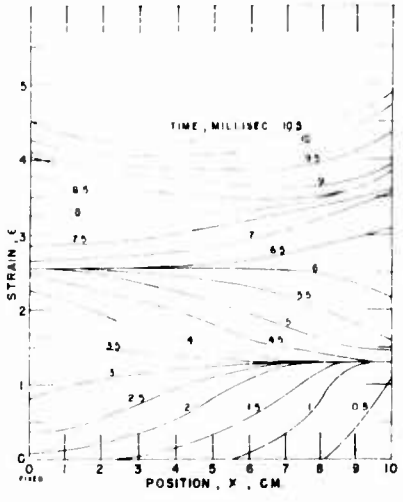

Figure 7. Rubber impact. Strain vs. Position for each flash of strobe light. Smoothed curves.

In order to have a measure of the slow-speed response, an Instron stress-strain curve was also run on the rubber. The velocity of the head for this test was 5 inches per minute for a 2-inch sample, or 250% per minute. Three specimens were measured and an average curve drawn (Figure 9). The average strain at break for the three was 548%. The average strain at break for three impact tests was 432%. (The three impact tests are the one shown (Figure 4) and two others for which the synchronization was not good enough for a complete picture but from which a measurement of the strain at failure could be made.) By "average" for an impact test we mean values averaged along the sample as well as for the three trials. From the strain-position curves (Figure 7) it is obvious that the strain at the position of the break is higher than the average along the string but apparently not as high as the strain at break in the Instron test.

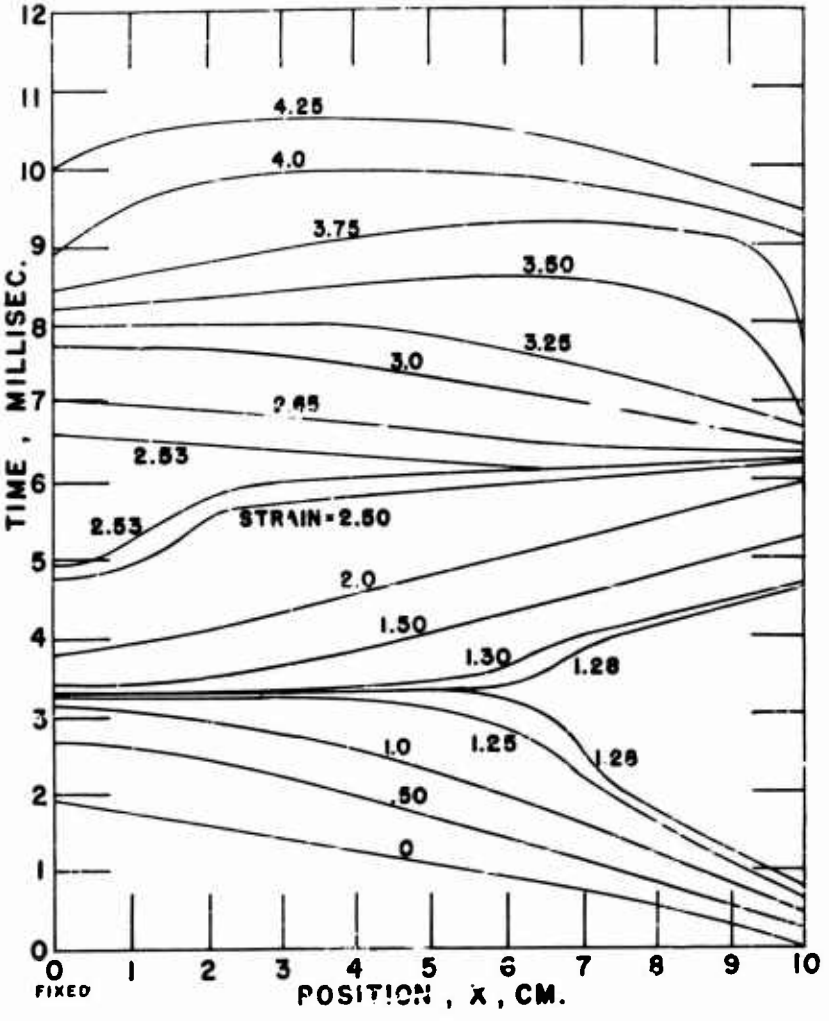

Figure 8. Rubber impact. Position vs. Time, showing lines of constant strain.

2. Dynamic stress-strain curve

The purpose of the analysis about to be described is to determine whether the response of the material may be wholly or partly defined by a dynamic stress-strain curve and, if so, to find the curve. If the response is only partly so defined, we will try to express in some way the manner in which it departs from it. To do this we must first fix on a stress-strain curve. Then we assume that this curve wholly defines the response and use von Karman's solution and method of characteristics [9-11] to calculate the strain waves. As we will see, such a curve only partly defines the response and we must include creep to get a reasonable picture.

For a first trial we might try the Instron curve but since we have some information from the data we should be able to develop a more appropriate curve. Before any reflection has taken place the reciprocal of the slope of a line in the (x,t) diagram is equal to the wave velocity, c, at that strain. Also we may determine the maximum value of the strain for the first pulse, ϵ_1, and we know the impact velocity, $v_.$. For the purpose of establishing the stress-strain curve, we will assume that the stress is a function of strain only and not of time, $\sigma = f(\epsilon)$, and then we may use the relation of von Karman,

$$v_1 = \int_0^{\epsilon_1} c\,d\epsilon .$$

We define the general parameter,

$$\phi = \int_0^{\epsilon} c\,d\epsilon ,$$

a point on which is given by $\phi = v_1$. A second point is given by the fact that the strain after one reflection is fairly well established. This will be at $\phi = 2v_1$. So we may construct the three curves, (ϵ,σ), (ϵ,c) and (ϵ,ϕ) using the relations

$$c = \sqrt{1/\rho\ d\sigma/d\epsilon}$$

and

$$\phi = \int_0^{\epsilon} c\,d\epsilon$$

and the few points determined as above.

This is shown in Table I. The numbers in boxes represent data. A smooth (ϵ, c) curve was drawn through the data points as far as possible (to $\epsilon = 1.28$) and an (ϵ, ϕ) curve calculated from it by integration. The curves were then adjusted so the (ϵ, ϕ) curve would pass through the point ($\epsilon = 1.28$, $\phi = 4.2$). Both curves were then continued smoothly in such a way that the (ϵ, ϕ) curve would pass through the point ($\epsilon = 2.53$, $\phi = 8.4$). Above this point the (ϵ, c) curve was drawn parallel to the (ϵ, c) curve calculated from the Instron (ϵ, σ) curve, but bending over at the top so it reached no higher value of c than the maximum value for the Instron curve. The thought behind this restriction on c is simply that although the dynamic values for c are higher than the corresponding Instron values at low strains, we have no reason to believe that when the rubber is rapidly strained to high values it is any more crystalline or in any condition to better support a high velocity of propagation than when slowly strained to high values. Values for σ were calculated from the finally-accepted (ϵ, c) curve. These curves are shown in Figures 9 and 10 along with the Instron curves.

3. Construction of response ignoring creep

In this first trial we assume that these curves completely define the response of the material and construct the pulses by the method of characteristics. The characteristic relations are $v \pm \phi$ = a constant where v is the particle velocity and $\phi = \int c\,d\epsilon$ as defined above. To aid in visualizing these characteristics we may plot them on a (v, ϕ) plane where v runs from zero to v_1 and ϕ from zero to as many multiples of v_1 as there are reflections. Obviously, on this plane the characteristics are straight lines at $\pm 45°$ slopes (Figure 11).

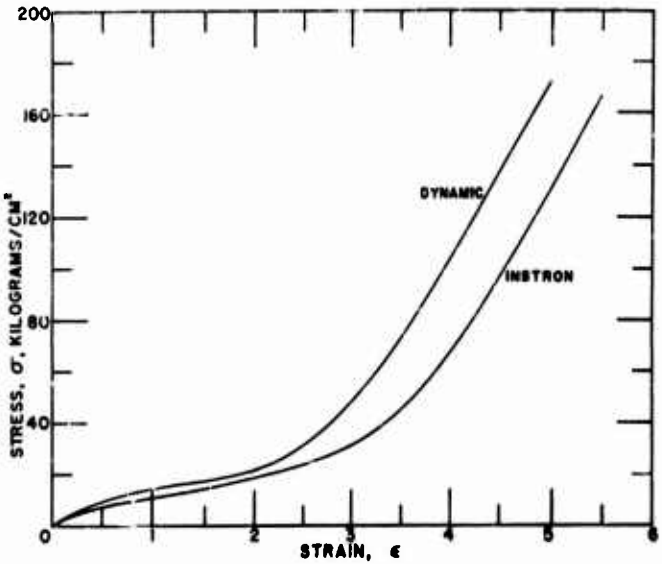

Figure 9. Rubber stress-strain curves.

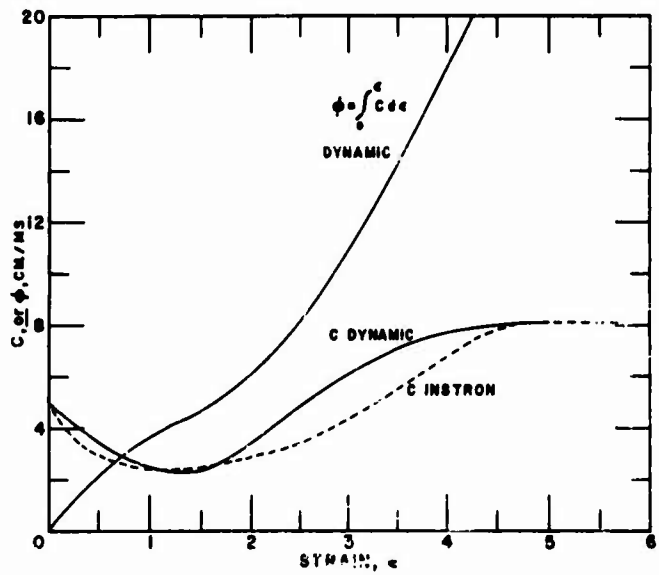

Figure 10. Wave velocity, c, for rubber, dynamic and Instron. Also dynamic ϕ.

TABLE I. DYNAMIC RUBBER VALUES

ϵ	c	$\phi = \int_0^\epsilon c\,d\epsilon$	$\sigma = \rho\int_0^\epsilon c^2 d\epsilon$
	cm/msec	cm/msec	gms/cm^2
0	5.0	0	0
.2	4.3	.93	4.8×10^3
.4	3.7	1.73	8.3
.5	3.39	----	----
.6	3.25	2.43	11.0
.8	2.8	3.03	13.0
1.0	2.74	----	----
1.0	2.45	3.56	14.5
1.2	2.3	4.03	15.7
1.28	2.0	4.2	----
1.4	2.28	4.49	16.9
1.6	2.48	4.96	18.1
1.8	2.90	5.50	19.7
2.0	3.43	6.14	21.9
2.2	3.96	6.87	25.0
2.4	4.54	7.72	29.0
2.53	----	8.4	----
----	----	----	----
----	----	----	----
----	----	----	----
5.0	8.10	25.96	172.5

Note: Numbers in boxes represent data.

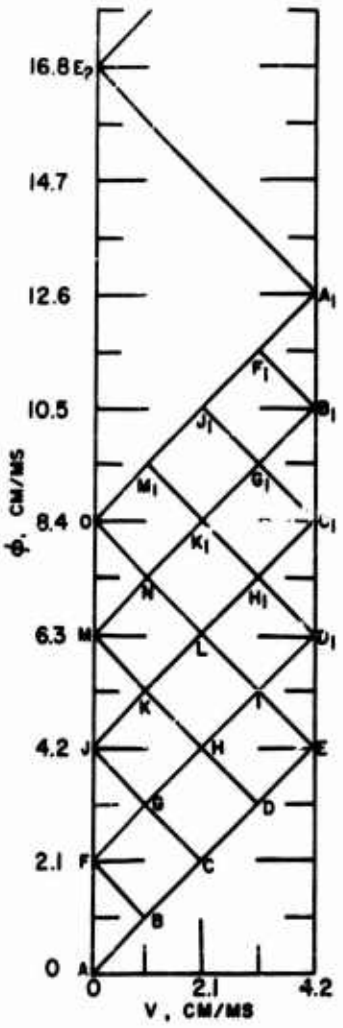

Figure 11. (v, ϕ) diagram for a rubber impact. v is particle velocity and $\phi = \int c\,dv$. Lines are characteristics, $v \pm c = a$ constant.

We then construct the response on an (x, t) diagram (Figure 12). Values for the points through the first reflection are given in Table II. Here we have allowed for the fact that the head takes a little time to accelerate and does not instantly start at v_1 as previously assumed. This is shown in the first five unlettered points in the table at $x = 10$. They are obtained by estimating a velocity-time curve for the head from the distance-time data (Figure 5). The first point is for $v = 0$ and the fifth point is for $v = v_1 = 4.2$, the maximum velocity of the head. Enough points are taken in between to give the desired detail in the construction. Since $\phi = v$ for the first pulse, values of ϵ corresponding to these points may be obtained from the (ϵ, ϕ) curve (Figure 10) and values of c from the (ϵ, c) curve (Figure 10). Straight lines are then drawn from these points at the slopes given by the values of c. These lines are straight until they meet reflections from the fixed end. The letters in Table II correspond to those in Figures 11 and 12.

Let us illustrate the method of finding the location of points

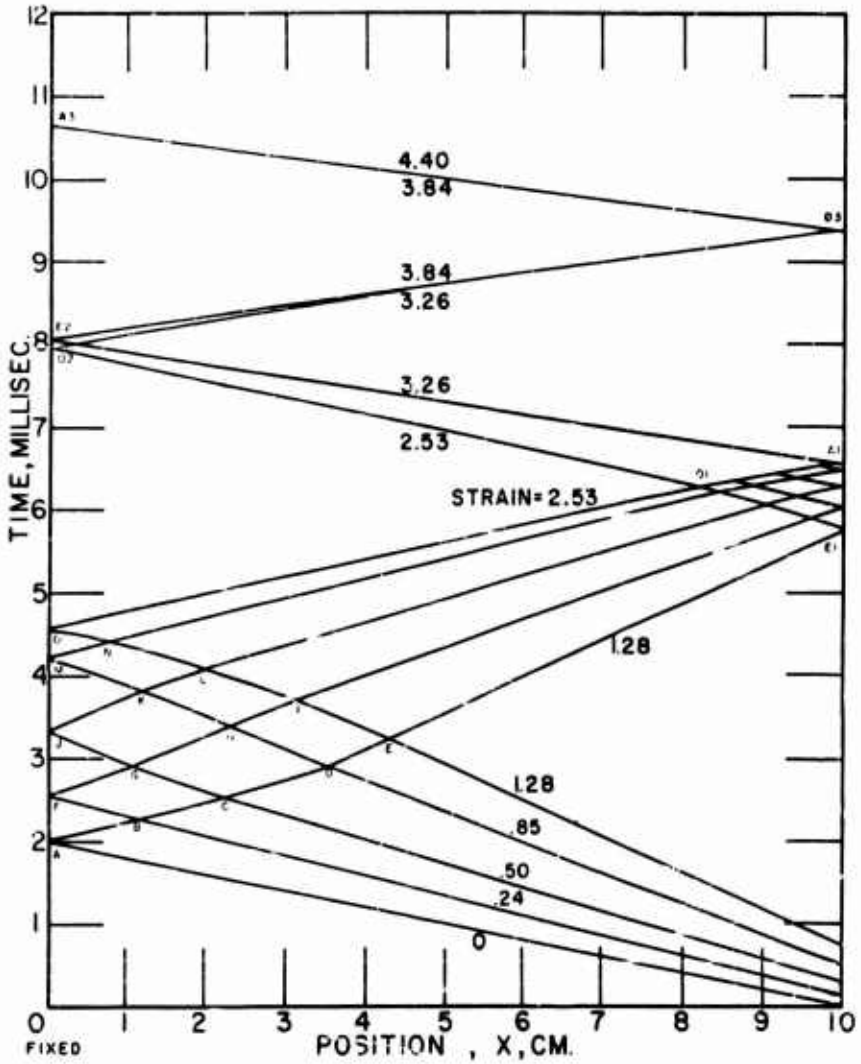

Figure 12. (x, t) diagram for a rubber impact calculated from characteristics. (x is position on the unstrained sample.)

TABLE II. CALCULATED STRAIN WAVE PATTERN IN RUBBER

Point*	x	t	ϵ	c	v	ϕ
	cm	msec		cm/msec	cm/msec	cm/msec
		0	0	5.0	0	0
		.13	.24	4.15	1.05	1.05
	10	.26	.50	3.45	2.1	2.1
		.51	.85	2.7	3.15	3.15
		.75	1.28	2.27	4.2	4.2
A	0	2.00	0	5.0	0	0
B	1.15	2.27	.24	4.15	1.05	1.05
C	2.22	2.53	.50	3.45	2.1	2.1
D	3.50	2.92	.85	2.7	3.15	3.15
E	4.32	3.26	1.28	2.27	4.2	4.2
F	0	2.57	.50	3.45	0	2.1
G	1.07	2.90	.85	2.7	1.05	3.15
H	2.34	3.39	1.28	2.27	2.1	4.2
I	3.18	3.72	1.72	2.70	3.15	5.25
J	0	3.34	1.28	2.27	0	4.2
K	1.22	3.83	1.72	2.70	1.05	5.25
L	2.04	4.09	2.05	3.56	2.1	6.3
M	0	4.22	2.05	3.56	0	6.3
N	.79	4.41	2.31	4.25	1.05	7.35
O	0	4.58	2.53	4.90	0	8.4

* Letters correspond to letters in Figures 11 and 12.

within the reflection. Suppose that we know the location of two points, one on a characteristic from the head and the other on a reflected characteristic from the fixed tail, and we wish to know where they will intersect on the (x,t) plane. From the (v,ϕ) diagram (Figure 11) we may determine the value of ϕ for the two known points and the unknown point of intersection. We then calculate the average value of ϕ between each of the points and the point of intersection and from that an average value of c between points and so we know the slopes from the known points and may determine the value of x and t at the intersection. We see that using average values in this way, the more of the intermediate strain values we use, the more accurate is our construction. After completing the first reflection, the pulse is again represented by straight lines until there is another reflection, this time at the head. This continues until the breaking strain is reached.

The results of this construction may be seen in Figure 12 and compared with the (x,t) plot of the data, Figure 8. The diagrams are on a slightly different basis in that all the lines in the data plot are constant strain lines, whereas in the constructed plot only the lines between reflections represent constant strain, and the crisscross lines within the reflections are characteristic lines. However, the strain is known at all points within the reflection and lines of constant strain could be constructed. They would be bounded by the outside lines of the reflection and be roughly parallel to the x-axis.

In comparing Figure 12 with Figure 8 we see that the constructed plot reproduces the data fairly well as far as the buildup of strain is concerned. In fact, if we plot strain against time for any one position, it looks quite reasonable. This has been done in Figure 13a where the solid experimental curve taken from Figure 8 may be compared with the calculated curve taken from Figure 12. But in considering the figures as a whole it is obvious that although the shape of the pulses and the size of the space-time area of constant strain agree fairly well for one pulse and its reflection, the changes with time of the wave form are in an opposite sense in the two figures. In the constructed plot the pulses become

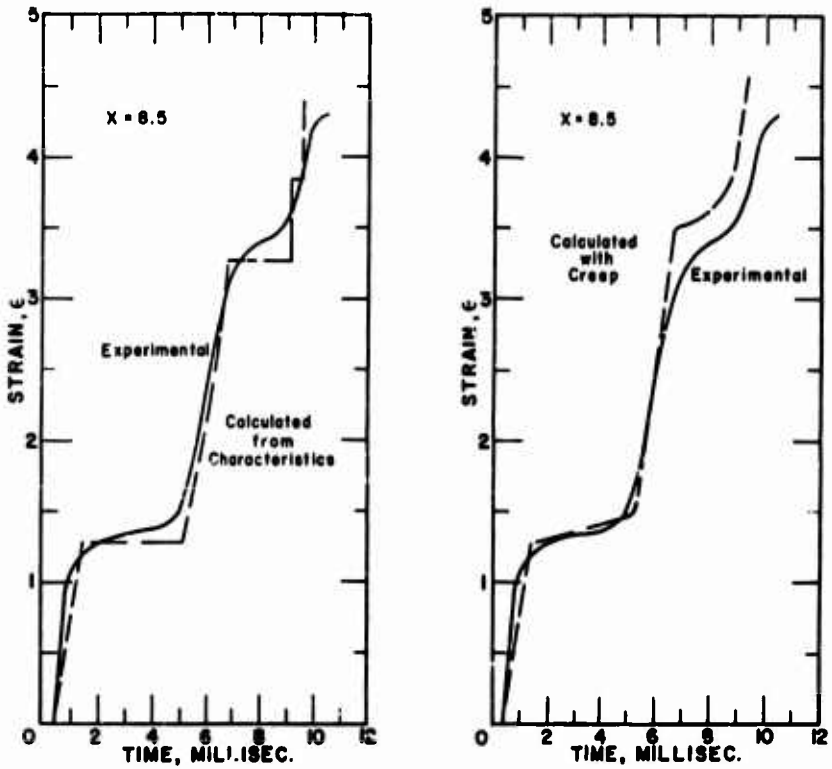

a. Experimental and calculated from characteristics.

b. Experimental and calculated with creep.

Figure 13. Strain vs. Time for one position (8.5) in the sample of impacted rubber.

sharper and the constant strain areas become more pronounced as time goes on, but in the data plot the pulses spread out so they are unrecognizable and the constant strain areas disappear. To further show that the picture we have constructed in Figure 12 is not correct, we look again at the (v, ϕ) diagram (Figure 11).

Here we see that the particle velocity in the constant strain areas near the fixed end is zero and near the head it is equal to v_1. From the original diagram of corrected data (Figure 5) we see this is true for only the early times indicated by the constant strain areas in the data (x,t) diagram (Figure 8).

4. Other possible constructions without creep

In trying to improve our constructed picture so that it gives a better match with the data, the first thought is whether we used the correct stress-strain curve. An effort was made to find a stress-strain curve that would give a better fit, but with little success. One such trial was made by constructing rather extreme and unnatural strain-velocity and stress-strain curves for which the only criterion as to how to draw the curves was to make the constructed (x,t) diagram of strain match the strain data. The result was an improvement over Figure 12 in the sense that the pulses did not sharpen up as much and did not quite reach the condition of being a shock wave. This is the condition at the top of Figure 12 where the calculated pulse is a single line. However the pulses still became sharper with time, rather than spreading out as in the data. If this procedure had given a picture that matched the data, we could accept the unnatural-seeming curves but if the improvement they give is minor, it seems better to stay with a more natural stress-strain curve and look for some other mechanism to explain the results.

In general, we may say that any stress-strain curve used in the manner described will give well-defined pulses and if the curve is at all concave upward the pulses will become sharper with time. If the curve bent downward so that the slope and therefore the wave velocity became less with greater strains, the pulses would tend to spread out, but then the whole picture would be quite different. With a lower wave velocity there would be more time between reflections. With more time between reflections there would be less interference between the pulses, and the slower wave velocities should appear as steeper lines of constant strain in the (x,t) diagram than appeared in the data. In fact, to reproduce the data entirely by wave motion, it would

appear that each pulse would have to have the complete spectrum of wave velocities from the fastest to the slowest. Some analyses were tried in which each successive pulse was treated as if it were progressing into previously unstrained material, but the results were not very satisfactory. Besides, no satisfactory mechanism for such behavior could be imagined.

Therefore it was concluded that a dynamic stress-strain relation alone will not explain the response of the material, and in order to get agreement we must consider that a certain amount of creep is taking place in the time of the experiment.

5. Construction with creep

Creep of rubber for short times has been investigated [12, 13]. Direct measurement is difficult but the behavior may be deduced by the principle of equivalence of time-scale and temperature change which is well established [15-17]. The creep strain is observed for measurable times at various temperatures. The values of strain at each time and temperature must then be normalized in such a way as to correct for the change in equilibrium strain with temperature. Conant, et al. [12], did this by expressing each strain as a percentage of the equilibrium strain at that temperature. Wood [13] used T/298 as a normalization factor where T is the temperature of observation in °K and 298°K (25°C) is a reference temperature. This procedure is based on the conclusions of the statistical theory of an equilibrium modulus of rubber elasticity [16]. The corrected strains may then be plotted against the logarithm of time and shifted along the log-time axis until the overlapping portions coincide. We then have a curve showing the creep of rubber at a single temperature. The curve is sigmoid in shape on a log-time scale. With times reduced to room temperature, the slope rapidly increases to a maximum at times of the order of microseconds, and then decreases and becomes linear on this log-time scale at times above a second or so.

It was not feasible to conduct the above experiments on the rubber used in the present investigation. It was assumed that a creep curve for this rubber would have the same general shape as

those published for other rubbers, particularly in the time scales of the changes in slope. Since in these curves the maximum slope is at times of the order of microseconds and the slope is linear at times greater than 1 second, the slope will not be changing rapidly in the time scale of the present experiment which is in the order of milliseconds. Therefore we will not be greatly in error if we consider the creep curve on a log-time scale to be linear for the less than 2 decades of time involved. What we shall do is determine the slope for some of the observed values in the early part of the experiment and consider that this holds throughout. As some support we may conduct a creep experiment at room temperature and see whether the slope is appreciably less than that determined as above. The equation for a creep that is linear on a logarithmic time scale is

$$\epsilon - \epsilon_o = k \log t/t_o .$$

A sample of the rubber used here was hung up under a steady load and the elongation observed as a function of time. The results are shown in Figure 14. The creep was logarithmic with a value of $k = .062$ using $\log_{10}$.

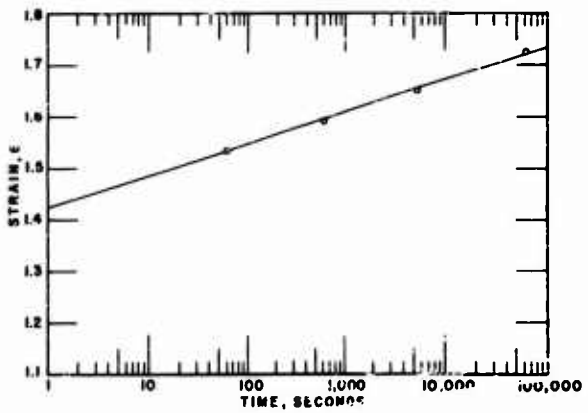

Figure 14. Creep of rubber.

From the data for the present impact experiment (Figure 8) in the time after the first pulse and before the second, the strain at the head, which should be constant according to the wave theory, rose from 1.28 at $t = 0.75$ millisec to 1.50 at $t = 5.25$ millisec. These values when substituted into the equation above give

k = 0.260 per decade. The creep rate thus calculated in the millisecond region is about four times as large per decade of time as the rate observed in the long-time experiment plotted in Figure 14. This is to be expected, for the sigmoid curve is steeper in the millisecond region than it is at longer times. So a logarithmic creep law with k = 0.260 will be combined with the above wave analysis to see if the agreement between Figure 12 and Figure 8 can be improved upon.

In using this logarithmic law, for each increment of strain for which we calculate creep, we must have a zero time when this strain first started and a later time when the strain value is known. (We must have a zero time in order to fix the time relation of the logarithmic creep with the rest of the experiment but there can be no zero on the logarithmic curve since that would imply a negatively infinite strain. What we are actually assuming is that the strain increases from zero strain and zero time on a sigmoid or some such curve and that in the region of interest we may approximate this curve by a logarithmic curve.) Creep was calculated for each pulse and also as a function of x. The beginning of the pulse, the time at each position when the pulse first had an effect, was taken as zero time for the creep due to this pulse and at this value of x. The other time used was the end of the pulse, the time when the strain at this position reached the maximum value of strain for this pulse as calculated without creep.

For each pulse there would be, on the (x, t) diagram (Figure 15), a line for the maximum value of strain without creep, and above this, lines at intervals for the creep to be added to this strain. For example, the maximum strain of the first pulse was 1.28, and lines were calculated for strains of 1.28 + .02, 1.28 + .07, and so forth. During the interval between the first and second pulses, only the creep resulting from the first pulse was present, but as soon as the second pulse had passed, the creep resulting from it was superposed on the creep already present. So at any point in the diagram the total strain at that position and that time is given by the sum of the strains contributed by all the pulses that have passed plus the amount by

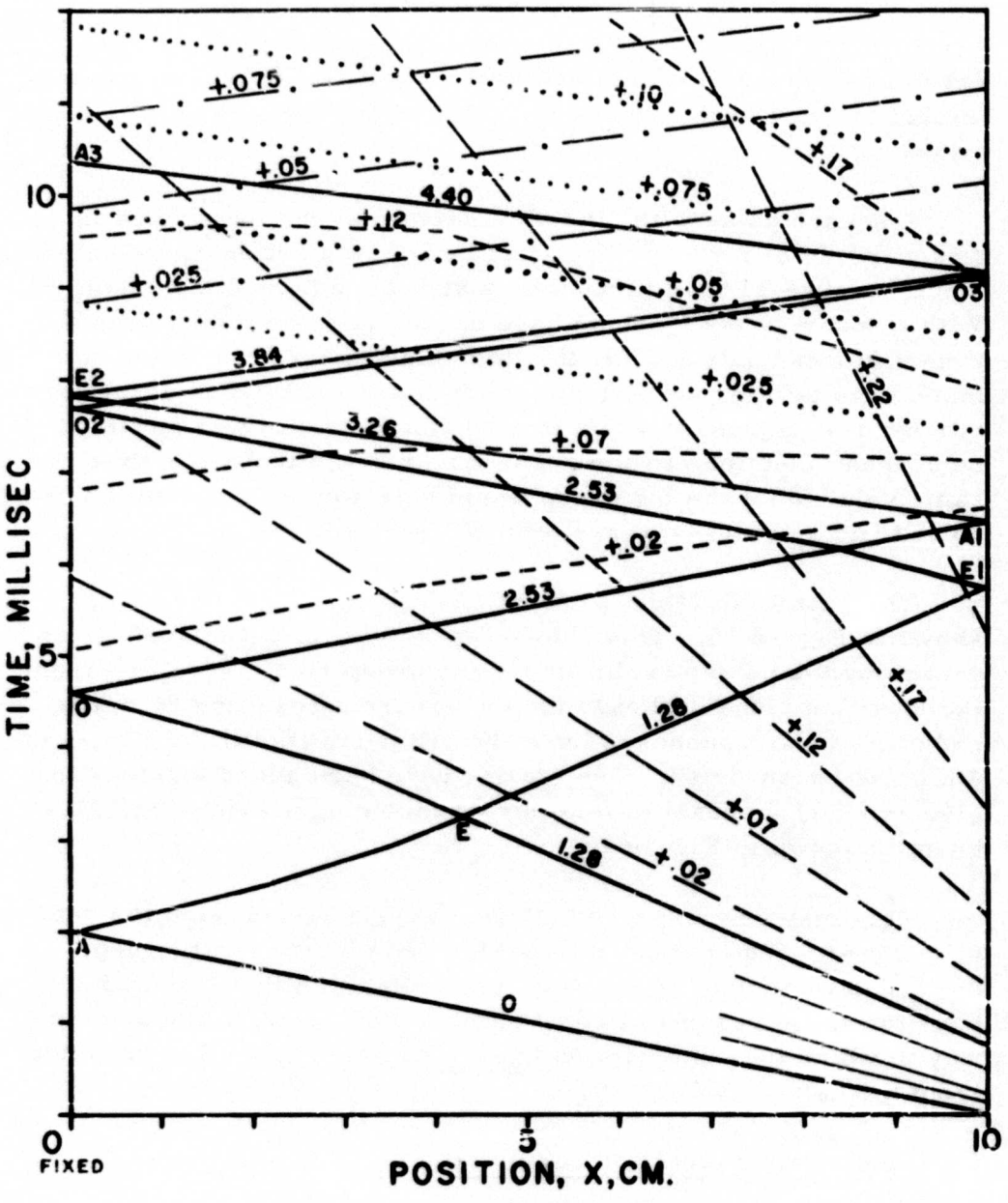

Figure 15. (x,t) diagram for a rubber impact. Solid curves are calculated from characteristics and the strain level is shown for each curve. All broken curves give the added strain due to creep, and the increment due to creep is shown for each curve.

which the strain contribution of each pulse has increased by creep since its passage. In calculating the characteristic lines, the creep was ignored within a reflection but it was included in determining the wave velocity and the slope of the lines between reflections.

A square pulse with a vertical front may not be handled in this way. In order to use a logarithmic law starting at the end of a pulse we would have to assume a zero time before the pulse. With a square wave front we have no way of determining such a time. In this analysis only the late pulses where there was not much time left had very steep fronts that made the use of the logarithmic law impractical. In this region the creep was assumed to be a linear function of time. The linear creep that gave about the same values that the log creep would have for the short times involved had a strain increase of 0.025 per millisec.

The results of taking account of creep in the analysis are shown in Figure 15. This shows separately the calculated strain caused by the pulses (solid line), the creep strain resulting from the 1st pulse (long dashes), the creep strain resulting from the 2nd pulse (short dashes), from the 3rd pulse (dots), and from the 4th pulse (dash-dots). The strains have been added together to give an (x,t) diagram of total strain including creep. This diagram is shown in Figure 16.

This may be compared with the (x,t) diagram from the data (Figure 8). We see that the constructed picture (with creep) does match the data fairly well, particularly in that it does not have the large regions of constant strain which were the principal way in which the construction without creep (Figure 12) departed from the data.

6. General comments and summary

Unfortunately it is not easy to look at these pictures (Figures 8, 12, 16) and compare them very critically. It is possible that other assumptions as to just how the strain varies with time would give as good a picture. Plotting strain against time for any one

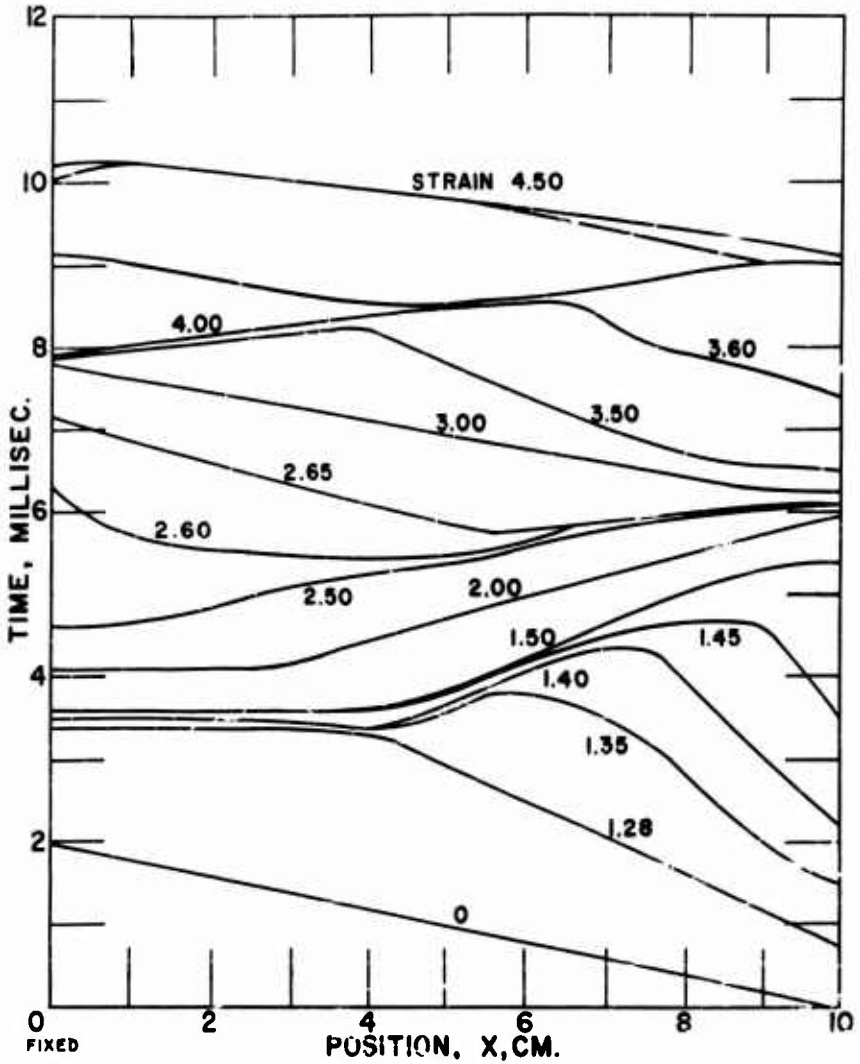

Figure 16. (x,t) diagram for a rubber impact obtained from Figure 15 by combining characteristic calculation and creep.

position does give a different point of view but is not completely satisfactory. For one thing, we must plot curves at fairly close values of x to be sure we have not missed anything. Also in comparing how two analyses match the data by the use of strain-time curves, it might be found that one analysis would match the data better for some values of x and the other match better for different values. In the present case the curves at a value of x = 8.5 were chosen as being fairly representative of all the curves. These are shown in Figure 13. As mentioned before, the construction without creep matched the data fairly well with this type of curve (Figure 13a). The construction with creep (Figure 13b) was better at first, but the calculated strain value rose above the data as the breaking strain was approached. This is probably because we oversimplified in assuming the same creep law to apply for the entire time of the experiment.

We shall review what we have determined concerning the response of a rubber strip to longitudinal impact. The over-all response and increase in local strain are wavelike in nature and in accordance with a stress-strain curve not very different from a slow-speed curve. However, the creep that occurs during the experiment is appreciable and must be considered. It tends to obscure the wave nature of the response.

PART III. NYLON YARN

When we discuss the nylon photographic data in a later section it will be seen that we have as yet been unable to get stroboscopic pictures of nylon impact accurate enough for an analysis, as has been done above for rubber. However, other measurements were made that will give some indication at least of how well a high-speed stress-strain curve characterizes the impact behavior of this material.

1. Result of time measurements with tail mass

First we will describe the use of a tail-mass method to determine a stress-strain curve. With a tail mass we determine force at the tail and average strain over the entire sample, both as a function of time. Strictly speaking, this will not give us a stress-strain curve when strain waves are present, since the stress and strain will not be measured at the same place at the same time. How well data obtained in this way represent the actual stress-strain curve for the nylon depends in part on the answer to our question as to how well a stress-strain curve characterizes the response of the material. If the stress-strain curve completely represents the response of the nylon, the wave fronts will be distinct and there will be no change in strain after the passage of a wave front and so the tail mass data would depart seriously from the stress-strain curve. However, if there is appreciable creep present, the increase in strain due to the waves will not be so large a percentage of the total increase as with wave motion alone. In this case the tail mass data will more nearly give the actual stress-strain curve. We will assume that there is sufficient creep so that these data may be called a stress-strain curve.

In order to use this stress-strain curve to compute a strain-wave pattern we must now ignore the creep. This is not contradictory to the above assumption, for here we are not assuming anything as to the actual behavior of the material but simply holding a variable constant in order to obtain a partial solution to a

problem. From this strain-wave pattern and the stress-strain curve we may determine a force-time curve for the tail end of the sample. This curve may be compared with measurements made by the weak link method (described later). If these measurements should agree with the computed curve, which must be thought of as a partial solution with no creep considered, it would indicate that there was no creep. However, this would be a contradiction, since we had to assume creep in order to accept the stress-strain curve. But we will see in the next section that the measured and computed curves do not agree and the computed curve does seem to be the partial solution that it should be.

Experiments performed:

A series of experiments with a tail mass were made on the high-tenacity nylon. The tail mass weighed 2.82 grams, the head mass 31.7 grams, the samples of nylon yarn were 27 1/2 inches long and the average initial head mass velocity was 160 feet per second. In a tail mass experiment, whether the sample breaks or not depends, among other things, on the velocity of impact. In these experiments, 160 feet per second just about strained the sample to the breaking point and some broke and some did not. About 60 shots were made and time-distance curves for the head and tail masses were determined, accurate to about ± 5% as in Figure 17. An Instron stress-strain curve (Figure 20) was taken on a 5-inch length of the nylon yarn at 12 inches per minute, or 4% per second for comparison with the results. Also the velocity of the first disturbance was measured by breaking a fine wire at the tail with no tail mass. This gave about 93 inches per millisec. So we may approximate the first strain pulse from

$$\frac{v_1}{c_0} = \frac{1.92}{93} = 2\% .$$

The average strain at any time may be determined directly from the position of the head and tail mass at that time and so a strain-time curve is as accurate as the distance-time curves. In order to obtain force or acceleration versus time we must

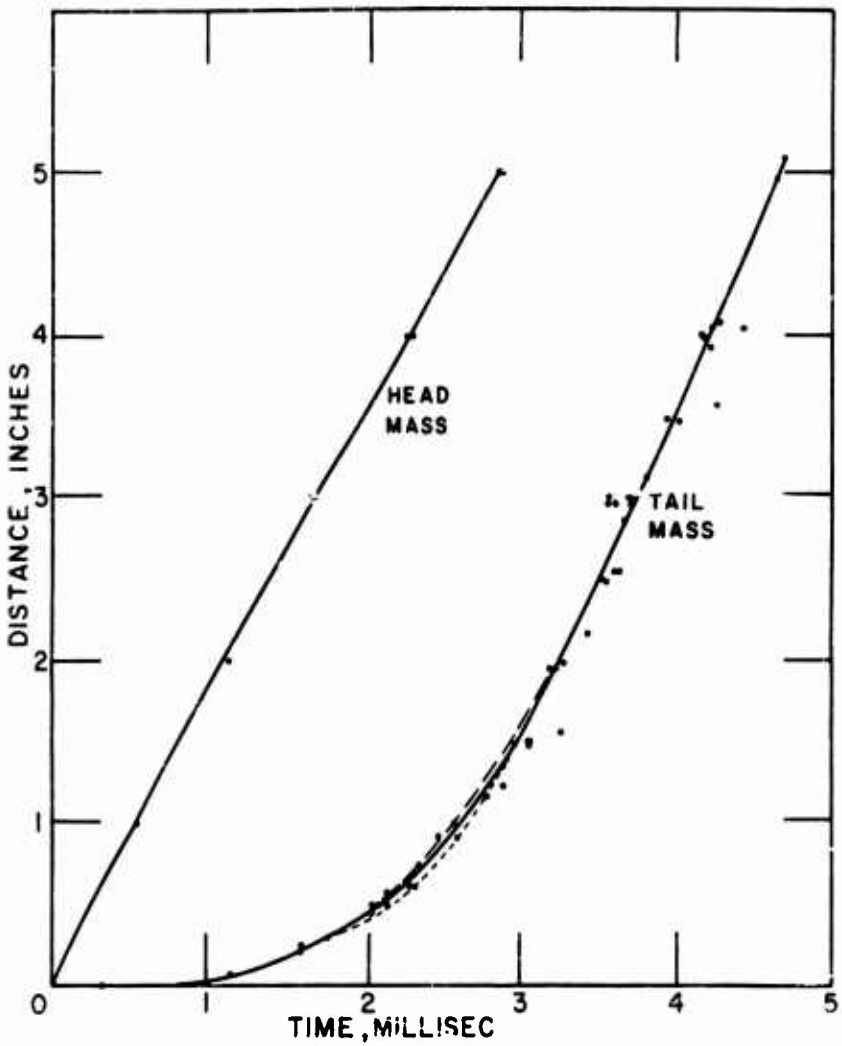

Figure 17. Nylon yarn impact. Position curves for 31.7-gram head mass impacted at 160 ft/sec and 2.82-gram tail mass connected with 27 1/2 inches of 1066 denier high-tenacity nylon yarn.

twice differentiate the distance-time curve of the tail mass. The results of such double differentiation are very dependent on the exact shape of the curve and the data were not accurate enough for very reliable results. However, some information was obtained.

Velocity and acceleration curves:

Uniformly-spaced points read from the distance-time curve of the tail mass were tabulated and numerically differentiated. The exact method of differentiation used did not seem to matter. Values of the derivative were plotted and a velocity curve drawn (Figure 18). Points from the velocity curve were then tabulated, differentiated and plotted to give the acceleration curve of Figure 19. Since the mass and acceleration of the tail mass are now known, the force acting on it may be calculated. This is the tensile force in the yarn at the point where it is attached to the tail mass.

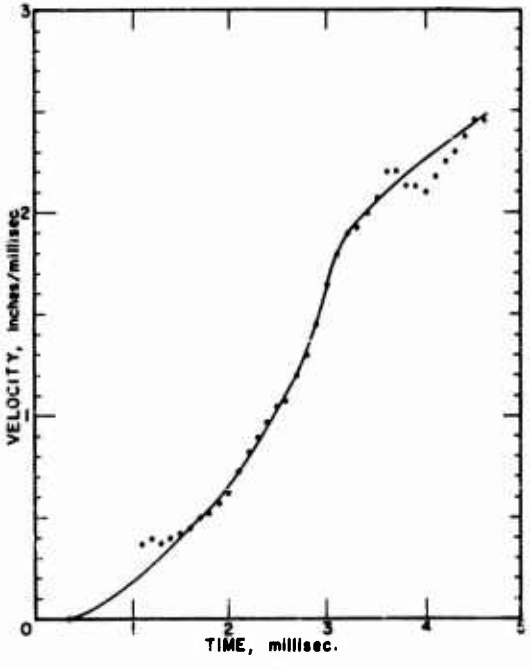

Figure 18. Velocity of tail mass shown in Figure 17.

There is some question as to just how the velocity and acceleration curves should be drawn. We could use the Instron stress-strain curve or some

assumed dynamic stress-strain curve and estimate where the wave motion would cause sudden changes of slope in the velocity curve and corresponding pulses in the acceleration curve. This could be kept in mind when drawing the curves through the plotted points of Figures 18 and 19. However, particularly since we are assuming an appreciable creep, it seemed better to draw the best smooth curve possible through the points and let the pulses form if they would. There was no definite evidence of pulses seen in this way. As we will see when discussing the photographs of strain waves, this agrees with the rounding and spreading of the pulses as they pass down the sample.

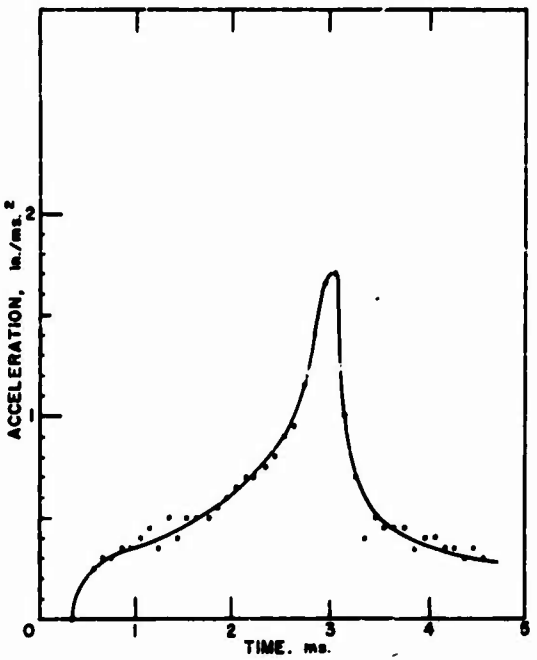

Figure 19. Acceleration of tail mass shown in Figure 17.

Stress-strain curves:

Stress, computed from such a smooth acceleration curve, was plotted against average strain as shown in Figure 20. This curve is only a little above the Instron curve at first but then rises sharply to about 160% of the maximum Instron stress at about 70% of the maximum Instron strain.

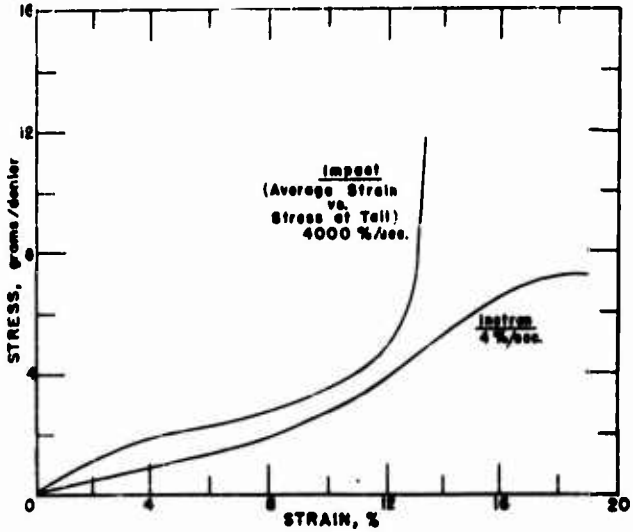

Figure 20. Stress-strain curves for nylon yarn.

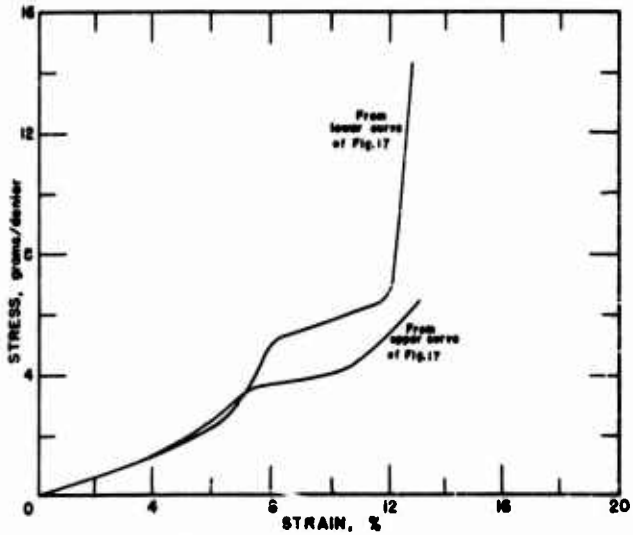

Figure 21. Stress-strain curves for nylon yarn calculated from extreme position curves to show improbable shapes.

In order to check these high stress values, the curve of tail-mass position in Figure 17 was redrawn in such a way as to lead to the most conservative possible estimate of maximum stress. The redrawn position lies above the original (solid) curve. The resulting stress-strain curve is shown in Figure 21. The maximum stress has indeed been reduced, but the curve has an irregular and improbable shape.

Going to the other extreme, still another curve of tail-mass position was drawn in Figure 17. This curve lies below the solid curve and gives the highest computed maximum stress. The stress-strain curve for this extreme is also shown in Figure 21. The maximum stress is twice the Instron value. Like the other curve in the figure, this one has an irregular and improbable shape. These various values are tabulated below.

TABLE III. MAXIMUM STRESS AND STRAIN VALUES FOR NYLON

	Max. stress (gm/denier)	Max. strain (%)
Instron	7.2	19.1
Impact:		
Lowest possible (from upper curve, Fig. 17)	6.6	13.3
Most likely (from solid-line curve, Fig. 17)	11.6	13.3
Highest possible (from lower curve, Fig. 17)	14.4	13.3

So we may say that the high-speed curve is definitely above the slow-speed one. The breaking strains are significantly lower with high-speed and the maximum stress at failure is probably significantly higher.

2. Result of time measurements with weak link

Measured stress pulse:

In measuring the force at the tail by the "weak link" method, the appropriate number of strands of AWG40 copper wire were held together and twisted with the end of the nylon. The joint was then coated with Pliobond cement. The joint was about 3/4 inch and the nylon sample was 30 inches long. The wire was placed in the tail clamp so as to leave 1/4 inch or less of free wire. An electrical connection was made from a wire within the joint and from the tail clamp so that when the free wire broke, the timing stopped. The timing was started by a wire immediately in front of the head mass. It was found by a static test that one strand of the AWG40 copper was broken by 137 grams. So by timing many tests with various numbers of strands and a new sample of nylon each time, a time profile of the force at the tail end of the sample could be determined.

This method could not be used for checking the maximum stress, as had been hoped. When there were more than about 30 wires so that their combined strength approached that of the nylon, the behavior was erratic and unreliable. However, the method seemed to work well with only a few wires and good measurement of the first pulse was obtained (Figure 22).

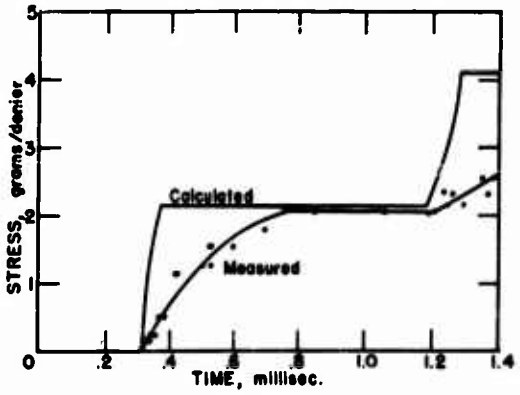

Figure 22. Stress pulse at fixed end of 1066-denier high-tenacity nylon yarn impacted at 160 ft/sec. Measured, and calculated from characteristics.

The initial increase in stress at the tail did not indicate a steep wave front but occurred

gradually. There was a definite plateau, however, before the second pulse reached the tail after reflection from the head.

Calculated stress pulse:

A theoretical study of the wave motion was made using von Karman's method of characteristics and the impact stress-strain curve shown in Figure 20.

The details of the analysis will not be given here, but the approach is about the same as with rubber. From the stress-strain curve, values of

$$c = \sqrt{\frac{1}{\rho} \frac{d\sigma}{d\epsilon}}$$

and

$$\varphi = \int_0^{\epsilon} c\,d\epsilon$$

are calculated. Then from the known value of the impact velocity of the head mass, 1.92 inches/millisec, the value of the maximum strain in the first pulse and the velocity of any strain in the pulse may be determined. Then by using the characteristic lines, the reflection at the tail may be computed, and so on. We now have an (x, t) diagram of the strain in the sample. By taking the values of strain and time at the tail and converting the strain to stress by the stress-strain curve, we obtain a calculated stress-time curve to compare with the measured curve from the broken wires. These are shown in Figure 22.

Comparison of measured and calculated curves:

The calculated stress-time curve agrees well with the data in the region of constant strain after the first pulse has passed. The theoretical value was 2.15 grams per denier and the value measured with breaking wires was 2.06 grams per denier.

However, the calculated initial wave front is much steeper than that observed. A study was made to make sure there were

no explainable factors causing this difference. The head mass does not actually assume the velocity v_1 instantly. Its acceleration was measured and this used to recalculate the shape of the first pulse. The (x,t) diagram for this calculation is shown in Figure 23. The same general type of response that is occurring in the nylon must occur in the wire link and it will take a finite time to reach breaking strain. The link was kept short so that this time would be short but it may be appreciable. The time to break the wires was estimated and this used to correct the experimental values.

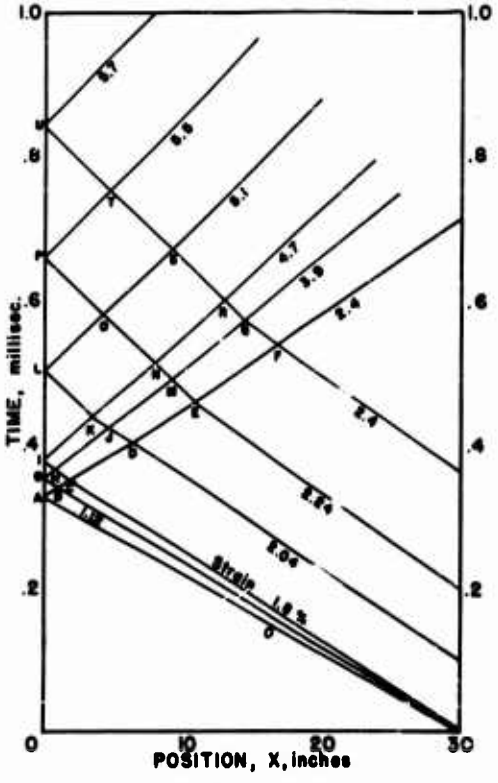

Figure 23. (x,t) diagram for a nylon impact at 160 ft/sec. Allowance is made for the time to accelerate the head mass.

Finally, for better comparison, the calculated stress values were adjusted so the plateau agrees exactly with the measured value. The results are shown in Figure 24.

The shapes of the curves are in fair agreement but the measured increase in stress is definitely slower than that calculated from a stress-strain curve. It does not seem likely that there could be a stress-strain curve that would give this slower increase and still give the good agreement in stress values on the plateau. Therefore there must be

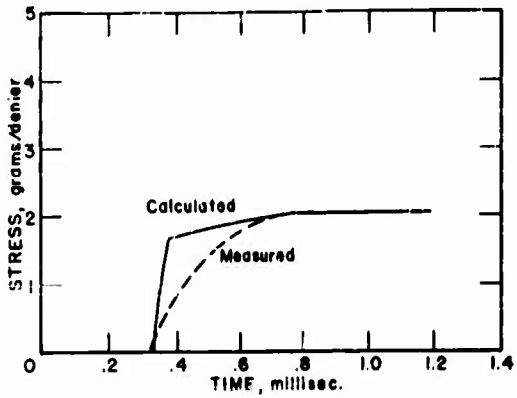

Figure 24. Stress pulse at fixed end of nylon yarn. As in Figure 22, except that measured values are corrected for time to break wires and calculated values are corrected for time to accelerate head mass and stress values normalized.

creep present to account for the difference in the curves. It might be better to call it "stress relaxation" in this instance but this is just another manifestation of the same mechanism as creep.

Summary:

To summarize, we may say that, for the first part of the curve where the weak-link method may be used, a stress-strain curve with the method of von Karman ignoring creep gives a good partial solution as seen by the agreement on the plateau, but for completeness we must include creep. However, there does not seem to be enough information here to evaluate the creep.

3. Reduction of photographic data

In the case of the rubber impact discussed in Part II the analysis would probably not be changed a great deal by an improvement in experimental accuracy. However, in Figure 6 we see that there is appreciable scatter in the strain data. This may be due to uneven illumination, lens distortion, film irregularity, fuzziness of the marks on being stretched, inaccuracy of the measuring microscope scale, or even non-uniformity of the material. In any case, with nylon yarn where the smaller cross section makes it much more difficult to get a good picture and the strains are much smaller, we can expect to have considerably more scatter in the nylon strain data. Since it will take considerable time and effort

to make an appreciable improvement in the experimental accuracy, we will discuss here what has been obtained so far and what steps have been taken to get as much as possible out of the data.

Picture of nylon impact:

The best picture of a nylon impact obtained is shown in Figure 25. This was made with a 75-cm sample of nylon yarn marked at every centimeter. There was an additional mark one-half centimeter beyond each 10-cm mark. It was impacted at 160 feet per second or 4.87 cm per millisec. The picture was taken at f/6.3 on Polaroid 3000 film and the stroboscope flashed at 6000 per second. Only about half of this sample was illuminated by the strobe. The white lines on the outside are calibration marks, 100 cm between inside edges. There were two white marks on the head mass and the straight lines made by them before impact may be seen in the upper right. The slanted lines across the whole picture are the streak made by the slider and the impact point may be seen about a third of the way down. Notice that the head moves a little faster than the slider. The break occurred at the head about three-fourths of the way down from the top of the picture. The illumination and picture quality were not uniform across the film and there were gaps in the data. Data are also missing from the part of the yarn hidden by the slider.

Measurements:

The position of each mark at each flash was measured with a measuring microscope and the reading corrected according to the distance between the 100-cm calibration points. The timing in the steady-light region was determined by moving straight across from the strobe region. From these corrected-position data, the length of each segment between marks could be determined at any time and so the strain at any time calculated. This procedure gave strain values with considerable scatter and it was obvious that some smoothing would have to be done before any use could be made of them. The strain could be calculated for greater intervals, say 5 cm, but this would be using only a fraction of the data available and trial calculations made in this way still seemed to have too much scatter.

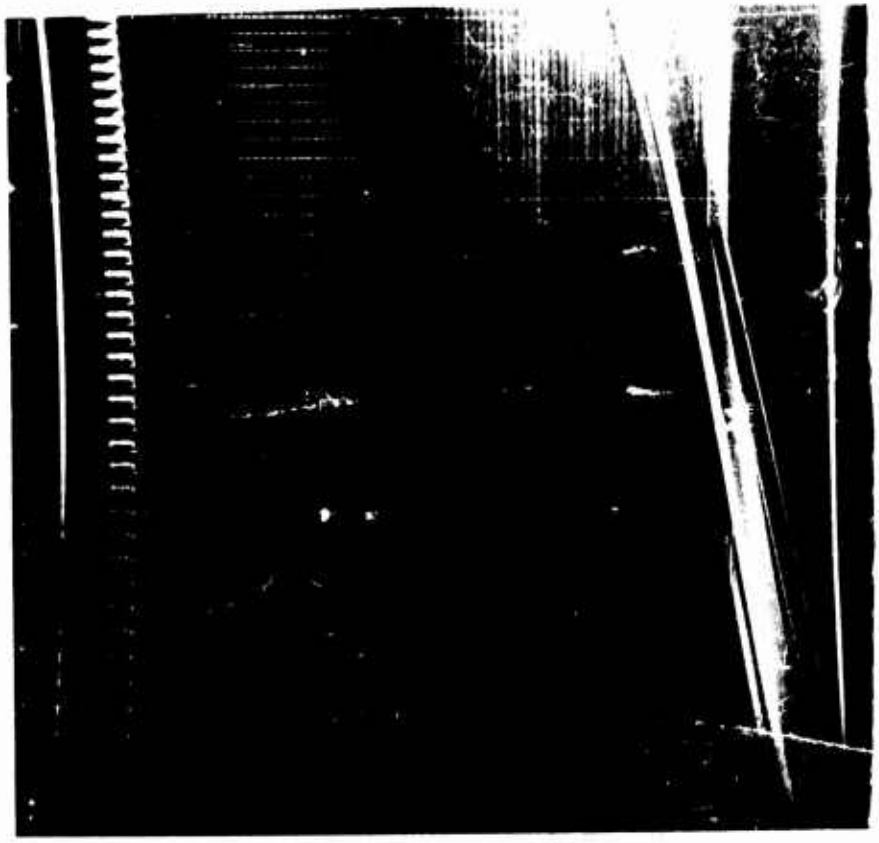

Figure 25. Nylon impacted at 160 ft/sec. 75-cm sample. Strobe rate 8000/sec. f/6.3 on Polaroid 3000.

Smoothing the data:

In order to use all the data and plot them in such a way that the variations could be smoothed out, the displacement of each mark from its original position was determined for each flash (i.e., time). For each flash the displacement was plotted as a function of the original unstrained position and a smooth curve drawn. This also served to fill in the gaps in the data. The displacement data and curves are shown for several flashes in Figure 26. The unit of time in all these curves is a flash and since the strobe operated at 8000 per second, eight flashes equal one millisecond or one flash equals one-eighth of a millisecond.

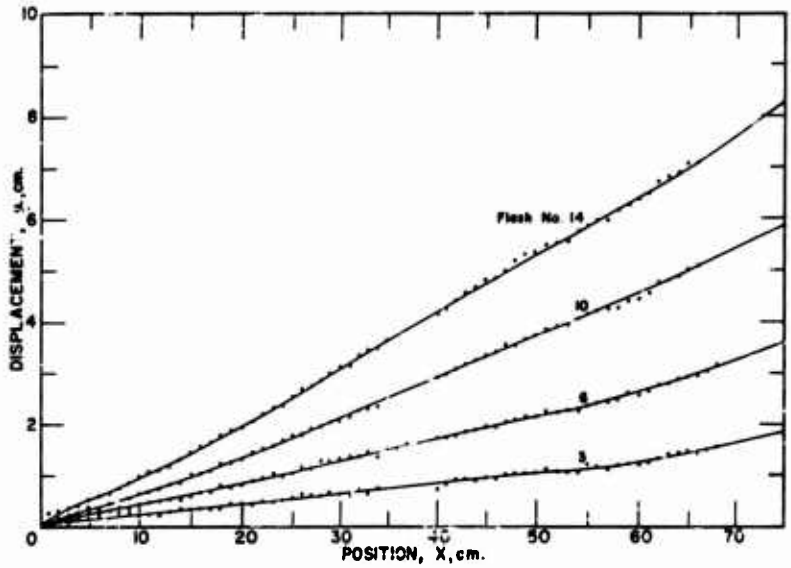

Figure 26. Nylon impact. Displacement vs. Position for several times (flashes), showing data and extent of smoothing required.

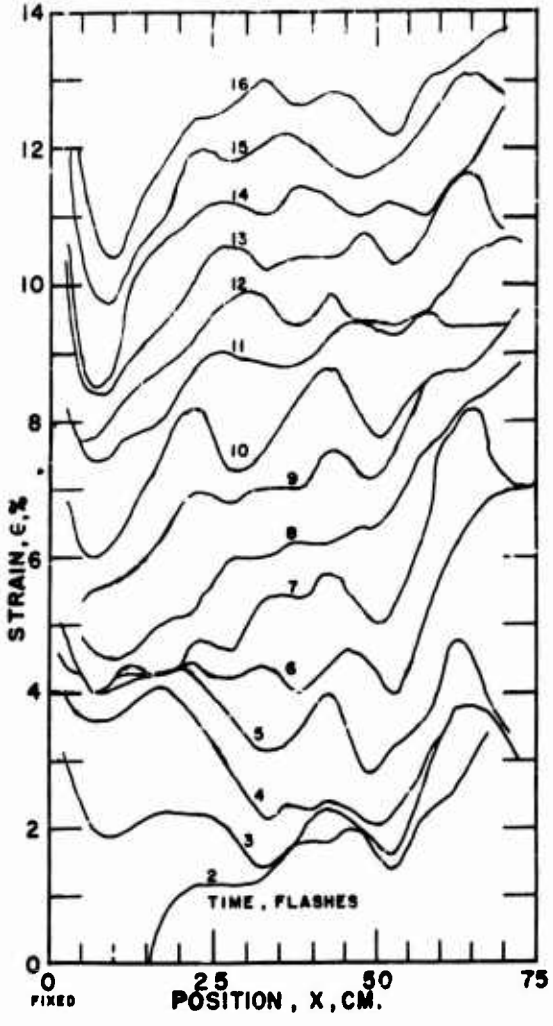

Figure 27. Nylon impact. Strain vs. Position for each flash. calculated from smoothed displacement curves as on Figure 26.

From the smoothed curves of displacement, u, as a function of position, x, the displacement was read at 5-cm intervals and tabulated. This was done for every flash. The strain is equal to $\partial u/\partial x$ which may be determined from this table. It was done with 5-point Lagrangian differentiation formulae but divided differences would give about the same results. The results are shown in Figure 27.

It had been expected that the graphical smoothing of the displacement curves would also smooth the strain values, but this was obviously not the case. It seems natural to assume that the extreme variations in each strain-position line are due to experimental error but we should consider the possibility that they are real. This will be discussed a little later.

Over-all response:

Even if these random variations of strain along the sample are real, they can be thought of as simply local perturbations if we wish to consider the over-all response of the material. For this purpose, we might wish to smooth them out. This could be done by drawing smooth curves through the points for each flash. However, the resulting curves would not be reliable enough to warrant the type of analysis that was tried with the rubber, and for general conclusions we may as well consider Figure 27 as is. Here we see that the lines for flashes 2 to 5 (.250 to .625 millisec) come together near the head with little change of strain and flashes 4 to 8 (.50 to 1.0 millisec) do the same at the tail. This behavior is most reasonably explained as a pulse building up at the head and being reflected at the tail. For greater times and strains there are no such well-defined regions and the strain merely increases with little or no evidence of pulses.

This means that the material is obeying a dynamic stress-strain curve at first, but at longer times creep becomes more important and obscures the wave nature of the response. This is the same general type of behavior that was observed with rubber.

Variations:

We now return to the question of whether the variations of strain with position observed in Figure 27 are entirely experimental error or to some extent at least are real. Some support for their reality is given by the conclusion of Stewart, et al. [4, 5], that similar variations observed by them were real. They subjected the same type of nylon yarn used here to transverse impact at ballistic speeds and recorded the longitudinal strain photographically. The variations in strain along the sample were similar to those observed here but with a greater amplitude and more closely spaced along the sample. They at first considered them to be errors, but after many tests concluded they were real. Before deciding whether our variations in strain are real or not, we must improve our experimental accuracy. Since this will take

some time, it seems worth while to try and draw a tentative conclusion from the present data.

Further smoothing of data:

What we must try to do is to find some means of smoothing the strain data that discriminates between random error and real variations. We could plot the strain as a function of time at different positions along the sample. The errors would appear in each curve but variations in strain due to position would be evident only in going from one curve to another. So drawing these curves smoothly would tend to smooth out errors However, the shape of the strain-time curves will depend very much on the shape of the wave fronts and how much creep is present. So their use would require approximations and assumptions that make this approach unsatisfactory.

It would be better if there were some other parameter besides strain that could be determined from the same measurements as strain, which would include the errors but which would not depend as much on the nature of the material at a given x-position as strain does. Particle velocity may be such a parameter. It is given by $v = \partial u/\partial t$ while strain is given by $\epsilon = \partial u/\partial x$. Therefore v can be calculated from the table of displacement values at different positions and times that was obtained from the smoothed (u, x) curves and used to calculate strain. Velocity should not be affected as much as strain by variations in the nature of the material along its length. For example, if there were a weak spot, the strain there might be much greater than on either side of this spot. But this spot could not be moving at a velocity that was much different from that of the adjacent material.

So particle velocity was calculated from the table as mentioned above and plotted against x for each flash, and smooth curves were drawn. In drawing these curves we took advantage of the fact that at all times the velocity at the tail is zero and at the head is equal to the velocity of the head mass. Some examples of the curves obtained are shown in Figure 28. The reasons given above for not smoothing strain by plotting it against time do not apply to

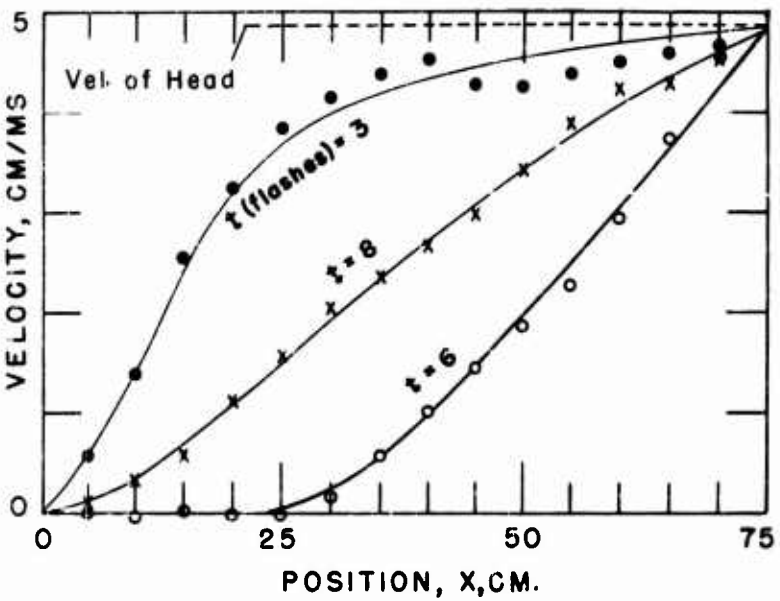

Figure 28. Nylon impact. Velocity vs. Position for several times (t), calculated from smoothed displacement curves as on Figure 26.

velocity, since velocity is not affected as directly by creep as strain is. Also the strain increases monotonically, but the velocity increases and decreases with the wave motion so that the wave motion is better defined. So for additional smoothing, values read from the smooth velocity-position curves may be plotted against time for each position and smooth curves drawn. Some examples are given in Figure 29. Here we see that the wave pattern is indeed evident for the entire time of the test and does not become obscured as the strain wave pattern does.

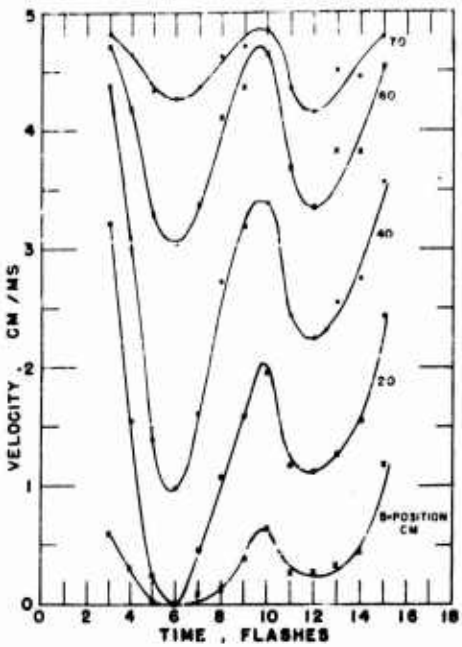

Figure 29. Nylon impact. Velocity vs. Time for several positions taken from smoothed velocity-position curves as on Figure 28.

From the smooth velocity-time curves a table of displacement values (u) was calculated by integration. From these the strain was computed. It is plotted in Figure 30 in the same form as Figure 27. Obviously we have not smoothed out the variations in strain at all; if anything, they are larger, but they are more regular. A dip in the strain occurs in the same x-position for the entire time of the test. This is the way we would expect variations in strain to appear if they were due to non-uniformity of the material (a local weakness, for instance).

Review of analysis of variations:

At this point we will review the successive methods that were used to analyze the data. The original position data taken every centimeter were plotted as displacement versus position for each flash and a smooth curve drawn. From these curves a table was made of the displacement every 5 centimeters. The velocity was calculated and plotted against position for each time. From these smooth curves values were taken to plot velocity against time and from these smooth curves velocity values were taken to integrate values for a new table of displacements. From this table strains were calculated and plotted in Figure 30. It is

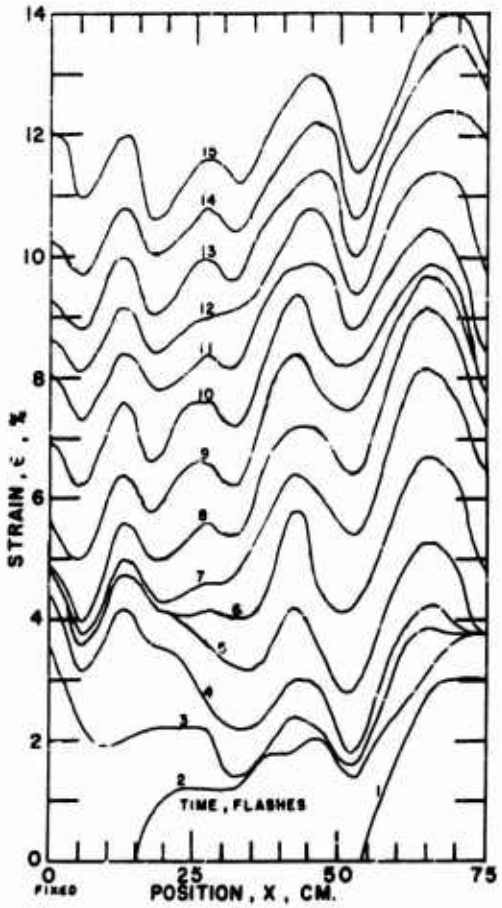

Figure 30. Nylon impact. Strain vs. Position for each flash calculated from smoothed velocity-time curves as on Figure 29.

hard to see how anything, real or random error, could survive all these steps. But there are reasons to believe that real variations would survive more readily than errors. Also it is hard to see how the steps taken could artificially produce the regular variations seen in Figure 30.

The conclusion is that the variations are real, but this must be considered only as a tentative conclusion, subject to confirmation as greater experimental accuracy is achieved.

Conclusion

We are seeking a system to explain the behavior of material in the form of strings or yarns when subjected to longitudinal impact, particularly when the velocity of impact and the size and nature of the sample are such that wave motion predominates in the response.

The first question is whether a dynamic stress-strain curve is useful and whether the behavior may be predicted using only a stress-strain curve and the wave equations as discussed by von Karman. The stress-strain curve is certainly useful and much of the behavior may be predicted in this way, as we may see from the strain-time curve for rubber, Figure 16, or the stress-time curve for nylon, Figure 22 or 24.

However, the dynamic stress-strain curve does not fully explain the behavior of the materials studied. This may be seen in the above figures or perhaps a little better for rubber by comparing the experimental (x, t) diagram (Figure 8) with that calculated from the stress-strain curve (Figure 12). Therefore any system of characterizing the behavior of the material based primarily on a stress-strain curve will have to include also a factor showing how the strain and stress vary with time alone while also varying with time and distance in the wave motion. This factor is presumed to be similar in nature to creep or stress relaxation. In Part II it was shown that use of creep significantly improved the calculated picture (Figure 16) in comparison with the experimental (Figure 8).

By the weak-link method with nylon we measured stress. Stress relaxation would slow up the increase in stress due to wave motion. This is seen to be the case (Figures 22 and 24).

The nylon strain data are considerably complicated by the variations in strain observed in the strain-position curves (Figures 27, 30). If the variations are real, they are probably due to variations in the strength of the material along its length. If this is so, it should be proper to average them out in studying

the over-all response. This was the approach taken by Stewart, et al. [4, 5]. In any case, there will have to be an improvement in experimental technique before we do more in this line.

Present plans are to improve the focusing of the stroboscope light, to use a larger camera lens so that more light will be focused on the film and so that larger film may be used, and to increase the size of the mirror to accommodate the larger lens. It would also help if a system could be devised to use a glass mirror with better reflective qualities than the metal one. It would increase the light intensity attainable from the strobe if a shorter sample were used. This would be acceptable if a greater impact velocity were used so that the number of reflections before break would be no more than at present. A significant improvement in picture quality might require a better measuring instrument than used so far. At present the uncertainty in the location of the marks in the picture is about matched by the limit of sensitivity of the measuring microscope.

When the quality of the strain data is improved, it may then be well to use other techniques simultaneously with the photographing of strain. For example, we might make a test with the sample marked for pictures but fastened to a tail mass rather than fixed. This would give us both strain data and force at the tail, from one picture. Or we might use a crystal-force gage to measure the force at the tail.

Although not yet ready for it, we should mention the ultimate step in work of this nature. Once we have arrived at the curves and equations that may be used to explain the response of a given material under a variety of conditions. we must then associate these curves and equations with the bonds, cross-linkages, entanglements, etc., that control the behavior of polymeric materials. This would not only contribute to basic understanding but also be useful for those trying to improve old materials or to develop new materials.

Acknowledgments

The author wishes to thank Dr. H. J. Hoge, under whose guidance both the experimental work and the preparation of the manuscript were performed. He also acknowledges the assistance of Mr. J. P. Ciccolo in particular for his preparation of the majority of the illustrations.

References

1. Schiefer, H. F., J. C. Smith, F. L. McCrackin, W. K. Stone, G. Fox, K. M. Towne, J. M. Blandford, P. J. Shouse, Stress-strain relationships in yarn subjected to rapid impact loading.

Part I: Equipment, testing procedure, and typical results, J. Research Natl. Bur. Standards, 54, 269 (1955).

Part II: Breaking velocities, strain energies and theory neglecting wave propagation, ibid., 54, 277 (1955).

Part III: Effect of wave propagation, ibid., 55, 19 (1955).

Part IV: Transverse impact tests, ibid., 57, 83 (1956).

Part V: Wave propagation in long textile yarns impacted transversely, ibid., 60, 517 (1958).

2. Authors and title as [1].

Part I: Textile Research J., 25, 520 (1955).

Part II: ibid., 25, 529 (1955).

Part III: ibid., 25, 701 (1955).

Part IV: ibid., 26, 821 (1956).

Part V: ibid., 28, 368 (1958).

Part VI: Velocities of strain waves resulting from impact, ibid., 30, 752 (1960).

Part VII: Stress-strain curves and breaking energy density for textile yarns, ibid., 31, 721 (1961).

Part VIII: Shock waves, limiting breaking velocities, and critical velocities, ibid., 32, 67 (1962).

3. Authors as [1]. [Condensed and selected versions of titles [1] and [2].]

a. Symposium on Impact Testing (1955) ASTM. STP No. 176, page 126.

b. Symposium on Speed of Testing (1956) ASTM. STP No. 185, page 47.

c. ASTM Bulletin, 220, 52 (1957).

d. J. Textile Inst., 50, T55 (1959).

4. Maheux, C. R., G. M. Stewart, D. R. Petterson, F. A. Odell, T. Hamburger, J. W. Jameson, Dynamics of body armor materials under high-speed impact.

Part I. Transient deformation, rate of deformation, and energy absorption in single and multilayer armor panels. U. S. Army Chem. Warfare Labs., Md., CWLR 2141 (3 Oct. 1957).

Part II. Single and triple microflash instrumentation for single yarn studies. CWLR 2142 (29 July 1957).

Part III. Dynamic strain-position distributions of nylon yarn impacted transversely. CWLR 2161 (14 Oct. 1957).

Part IV. Nominal dynamic stress-strain curves. CWLR 2184 (22 Oct. 1957).

Part V. Moving image photography for determining strain history in yarns. CWLR 2185 (30 Oct. 1957).

5. Petterson, D. R., G. M. Stewart, F. A. Odell, C. R. Maheux. [Nearly complete version of [4] with some additional comments.] Textile Research J., 30, 411 and 422 (1960).

6. Brinkworth, B. J., The propagation of strain in textile cables under longitudinal impact. Proc. Conf. Properties of Materials at High Rates of Strain, page 184. Inst. Mech. Engrs., London, 1957.

7. Meredith, R., The effect of rate of extension on the tensile behavior of viscose and acetate rayons, silk and nylon, J. Textile Inst., 45, T30 (1953).

8. Lewis, G. M., A method for the investigation of the stress-strain behavior of fibers at very high rates of extension. Proc. Conf. Properties of Materials at High Rates of Strain, page 190. Inst. Mech. Engrs., London, 1957.

9. Von Karman, T., On the propagation of plastic deformation in solids, OSRD No. 365 (1942), NDRC Report No. A-29.

10. Von Karman, T., H. F. Bohenblust, D. H. Hyers, The propagation of plastic waves in tension specimens of finite length, theory and methods of integration, OSRD No. 946 (1942), NDRC Report No. A-103.

11. Von Karman, T., P. Duwez, The propagation of plastic deformation in solids, J. Appl. Phys., 21, 987 (1950).

12. Conant, F. S., G. L. Hall, W. J. Lyons, Equivalent effects of time and temperature in the shear creep and recovery of elastomers, J. Appl. Phys., 21, 499 (1950).

13. Wood, L. A., The elasticity of rubber, J. Wash. Acad. of Sci., 47, 281 (1957).

14. Stuart, H. A. (Ed.), Die Physik der Hochpolymeren:4, Theorie und Molekulare Deutung Technologischer Eigenschaften von Hochpolymeren Werkstoffen, Springer-Verlag, Berlin, 1956.

15. Ferry, J. D., Structure and Mechanical Properties of Plastics, Chapter 6 in Reference 14 [in English].

16. Treloar, R. G., The Physics of Rubber Elasticity, Oxford Univ. Press, London, 1958.

17. Tobolsky, A. V., Properties and Structure of Polymers, John Wiley and Sons, Inc., New York, 1960.

DISTRIBUTION LIST

GENERAL STAFF

1 Deputy Chief of Staff for Logistics
Department of the Army
Washington 25, D. C.

1 Deputy Chief of Staff for Personnel
Department of the Army
Washington 25, D. C.

1 Deputy Chief of Staff for Military
Operations, Department of the Army
Washington 25, D. C.

1 Chief of Research & Development
Department of the Army
Washington 25, D. C.

ARMY

5 The Quartermaster General
Department of the Army
Washington 25, D. C.

2 Commanding General
Philadelphia QM Depot, U.S. Army
2800 South 20th Street
Philadelphia, Pa.

4 Commandant
QM Food & Container Institute for the
Armed Forces, U. S. Army
1819 W. Pershing Rd.
Chicago, Illinois

3 Commanding Officer
QM R&E Field Evaluation Agency, U.S. Army
Ft. Lee, Virginia
Attn: Chief, TSO

2 QM Liaison Officer, WCOL-8
Wright Air Development Center
Wright-Patterson AF Base
Dayton, Ohio

1 Commandant
The QM School
Ft. Lee, Virginia
Attn: Library

1 Commanding General
Frankford Arsenal, Phila 37, Pa.
Attn: Engr. Psychology Div. (L3)

3 Hqs., Army Electronic Proving Ground
Ft. Huachuca, Arizona
Attn: Aviation & Meteorological Dept.
Tech. Information Br.
Deputy Chief for Meteorology

2 Commanding General
The Engineer Center
Ft. Belvoir, Va.

1 Commanding Officer
Diamond Ordnance Fuze Labs.
Washington 25, D.C.
Attn: Tech Reference Section
(ORDTL-012)

2 Commanding General
Aberdeen Proving Ground
Aberdeen, Maryland

2 Chief Signal Officer
Department of the Army
Washington 25, D. C.
Attn: Res. & Dev. Div.

ARMY (Cont)

1 Commanding Officer
Signal Corps Engr. Lab.
Ft. Monmouth, N. J.

1 Office of Chief of Engineers
Department of the Army
Temp. Bldg. T-7, Gravelly Point
Washington 25, D. C.
Attn: Research & Dev. Div.

4 CO, Chemical Warfare Laboratories
Army Chemical Center, Maryland
Attn: Technical (AS 18) Library

1 Chief Chemical Officer
Department of the Army
Bldg. T-7, Gravelly Point
Washington 25, D. C.
Attn: Res. & Dev. Div.

2 CO, Hq., Medical Nutrition Lab.
Fitzsimons Army Hospital
Denver, Colorado
(1-Dr. Friedmann)

1 Armed Forces Institute of Pathology
Washington 25, D. C.

1 Chief, Armed Services Medical
Procurement Agency
64 Hoyt St., Brooklyn 1, N. Y.
Attn: Property Officer
Marked: Req. DUSD (H&M

1 Chief of Transportation
Department of the Army
Temp Bldg. T-7, Gravelly Point
Washington 25, D. C.

2 Commanding Officer
Transportation Res & Eng Command
U. S. Army
Ft. Eustis, Virginia
Attn: Tech Services Div.

1 The Army Library
Pentagon Bldg.,
Washington 25, D. C.

1 Commandant, Command & General Staff
College
Ft. Leavenworth, Kansas

1 Commandant, U. S. Military Academy
West Point, New York

1 Commanding Officer, Detroit Arsenal
28balk Van Dyke St., Centerline, Mich.
Attn: Res & Engr. Div.

1 Commanding General
Hqs., U.S. Army Medical R&D Command
Main Navy Bldg.
Washington 25, D. C.
Attn: MPAPP Research Branch

2 Commander
QM Intelligence Agency, U.S. Army
Washington 25, D. C.

2 Executive Director
Military Clothing and Textile Supply Agency
2800 S. 20th St., Phila. 45, Pa.

1 Commanding Officer
QM R&E Field Evaluation Agency, U.S. Army
Airborne Systems Test Div.
Yuma Test Station
Yuma, Arizona

ARMY (Cont)

1 Commanding Officer
Cold Weather & Mountain Indoctrination
School
Fort Greeley, Alaska

1 Commanding Officer
Fort Greeley, Alaska
Attn: Post Library

AIR FORCE

2 Department of Air Force
Hqs., USAF, Wash 25, D. C.
(1 DC/S materiel, 1 DC/S Dev.)

1 Director
Air University Library, Attn: 7575
Maxwell AFB, Alabama

2 Commandant
USAF School of Aviation Medicine
Randolph AF Base
Randolph Field, Texas

1 Commander, Arctic Aeromedical Lab
APO 731, Seattle, Washington

1 Commander
Air Res & Dev Command
Attn: RDSTL (Hqs., Tech Lib. Br.)
Andrews AF Base, Washington 25, D.C.

1 Commander
Wright Air Development Center
Wright Patterson AF Base, Ohio
Attn: Tech Library

1 Commander
Strategic Air Command
Offutt AF Base, Nebraska

1 Chief, Nutrition Div.
Air Development Center
Aero-Medical Lab.
Wright Patterson AFB, Ohio
Attn: Dr. Harry C. Dyme

1 Commander
AF Cambridge Research Center
Air Research & Development Cmd.
Laurence G. Hanscom Field
Bedford, Mass.
Attn: CRTOTT-2

NAVY

1 Director
Naval Research Laboratory
4th & Chesapeake St., S. W.
Washington 25, D. C.

1 Chief, Bureau of Ordnance
Department of the Navy
Washington 25, D. C.
Attn: R&D Div.

1 Naval Medical Research Institute
National Naval Med. Res. Center
Bethesda, Md.

2 Chief of Naval Research
Washington 25, D. C.
Attn: Code 4028

1 Chief, Bureau of Ships
Department of the Navy
Washington 25, D. C.
Attn: Code 338

1 Chief, Bureau of Med. & Surgery
Dept. of the Navy, Wash 25, D. C.
Attn: Code 33

NAVY (Cont)

1 Commander, U. S. Naval Ord. Test
Station, China Lake, Calif.
Attn: Code 753

1 Chief, Bureau of Aeronautics
Dept. of the Navy, Wash 25, D. C.
Attn: Code AE 52

1 Chief, Bureau of Supplies & Accounts
Department of the Navy
Washington 25, D. C.

CONARC

1 C O., U.S. Continental Army Command
Ft. Monroe, Va.

1 President
U. S. Army Artillery Bd.
Ft. Sill, Okla.
Attn: ATBA

1 President
US Army Armor Board
Ft. Knox, Ky.
Attn: ATBB

1 President
U. S. Army Infantry Bd.
Ft. Benning, Ga.
Attn: ATBC

1 President
U. S. Army Air Defense Bd.
Ft. Bliss, Texas
Attn: ATBD

President
U. S. Army Airborne and Electronics Bd.
Ft. Bragg, N. C.
Attn: ATBF

1 President
U. S. Army Aviation Bd.
Ft. Rucker, Ala.
Attn: ATBG

1 Commanding Officer
U. S. Army Arctic Test Board
Ft Greely, Alaska
Attn: ATBE

BOARDS & COMMITTEES

1 Army Committee on Environment
Chief, Research & Development
Pentagon, Washington, D. C.

1 Armed Forces Pest Control Bd.
Walter Reed Army Med. Center
Forest Glen Annex
Main Bldg.
Forest Glen, Maryland

1 Army Research Committee
Chief, Research & Development
Pentagon, Washington, D. C.

MISCELLANEOUS

1 National Research Council
2101 Constitution Ave., Washington, D.C.
Attn: Advisory Bd. on QM R&D

10 Armed Services Technical Information Agency
Arlington Hall Station
Arlington 12, Va
Attn: TIPDR

2 Gift and Exchange Division
Library of Congress
Washington 25, D. C.

1 U. S. Department of Commerce
Weather Bureau Library, Washington, D.C.

1 Central Intelligence Agency
Collection & Dissemination
Washington 25, D.C.

1 National Library of Medicine
Washington 25, D. C.

1 Generalintendanten
Standardiseringskontoret
Festningen
Oslo, Norway

1 Marine Corps Equipment Board
Marine Development Center
Marine Corps School
Quantico, Va.

1 Office of Technical Services
U. S. Department of Commerce
Washington 25, D.C.
Attn: Tech Rpts Sec (THRU OQMG)

1 U. S. Department of Agriculture Library
Washington 25, D. C.

1 Commandant
Industrial College of the Armed Forces
Ft. McNair, Washington 25, D. C.

1 QM Representative
Army Command and General Staff College
Department of the Infantry Div.
Ft. Leavenworth, Kansas

ADDITIONAL DISTRIBUTION

Dr. Jack C. Smith
Polymer Physics Section
National Bureau of Standards
Washington 25, D. C.

Dr. Herbert F. Schiefer
National Bureau of Standards
Washington 25, D. C.

Mr. George M. Stewart
Biophysics Division
Army Chemical Center
Maryland

Prof. E. H. Lee
Dept. of Applied Mathematics
Brown University
Providence, R. I.

Dr. Sudhir Kumar
US Army Research Office, Durham
Box CM, Duke Station
Durham, North Carolina

Mr. George J. Hasslacher, III
Dept. of Engineering Mechanics
Pennsylvania State University
University Park, Penn.

Mr. W. James Lyons
Textile Research Institute
Princeton, New Jersey

Mr. Mehmet Yontar
American Radiator and Standard
Sanitary Corp.
Research Division
Monroe and Progress Streets
Union, New Jersey

Mr. Joseph M. Krafft
Naval Research Laboratory
Washington 25, D. C.

Prof. Stanley Backer
Textile Division
Dept. of Mechanical Engineering
Massachusetts Institute of Technology
Cambridge 39, Mass.

Mr. Jan Krizik
Materials Technology, Inc.
15 Erie Drive
Natick, Mass.

Mr. Mark L. Dannis
Senior Research Associate
B. F. Goodrich Research Center
Brecksville, Ohio

Mr. Henry Morgan
KLH Research & Development Corp.
30 Cross Street
Cambridge, Mass.

Dr. Lawrence A. Wood
National Bureau of Standards
Washington 25, D. C.

Mr. W. Julian Ferguson
Naval Research Laboratory
Washington 25, D. C.

Prof. Prescott D. Crout
Mathematics Dept.
Massachusetts Institute of Technology
Cambridge 39, Mass.

Mr. John Jameson
Biophysics Division
Army Chemical Center
Maryland

E. I. du Pont de Nemours & Co.
"Dacron" Research Laboratory
Kinston, North Carolina
Attn: Mr. Louis G. Boccetti, Librarian